Centre for Ecology and Hydrology
Benson Lane
Wallingford
Oxfordshire, OX10 8BB, U.K.
8th Febraury 2017

Email: chg@ceh.ac.uk

To: Dr Astrid Kerkweg, Executive Editor of GMD

Dear Executive Editor

Response to reviewers' comments and editorial interactive comment for manuscript: gmd-2016-221:

Climate pattern scaling set for an ensemble of 22 GCMs – adding uncertainty to the IMOGEN impacts system (by P. Zelazowski, C. Huntingford, L.M. Mercado and N. Schaller)
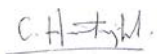
Thank you for arranging reviews for our manuscript, and in addition editorial comment. We have revised the manuscript to reflect in full the requested changes. In particular, for reviewer two, we have made a comparison – in terms of impact of runoff changes – using direct GCM projections against those using the IMOGEN system that emulates that model. The manuscript now has a new Figure 7 to present that, in addition to the related text.

We have responded to all requests. Please find below a list of each suggested amendment, and below each and in indented text are our responses and listing of any revised text in the manuscript itself.

Additionally at the bottom of this letter is a version of both the main manuscript and supplementary information, with "track changes" switched on to show our edits and changes.

Please do not hesitate to contact me if you have any further questions.

Yours sincerely,

C.H=tyM.

Dr Chris Huntingford (and on behalf of co-authors)

1

Response to gmd-2016-221-SC1 (Interactive comment from A. Kerkweg, Executive Editor).
Please note that some internal numbering from the review has changed slightly as review comments have been incorporated.

5

Comment 1.1. Dear authors, in my role as Executive editor of GMD, I would like to bring to your attention our Editorial version 1.1:
http://www.geosci-model-dev.net/8/3487/2015/gmd-8-3487-2015.html.
This highlights some requirements of papers published in GMD, which is also available on the
10   GMD website in the 'Manuscript Types' section:
http://www.geoscientific-model development.net/submission/manuscript_types.html

Response 1.1. Thank you for this and other comments. We have familiarised ourselves with the Editorial.
15

C.1.2. In particular, please note that for your paper, the following requirements have not been met in the Discussions paper:
The main paper must give the model name and version number (or other unique identifier) in the title.
20

R.1.2. We have added the version number, and as IMOGEN vn 2.0. This makes a clear distinction from vn 1.0, which was only calibrated against the United Kingdom Met Office model, HadCM3. This distinction is also noted in the main body of the text.

25   C.1.3. If the model development relates to a single model then the model name and the version number must be included in the title of the paper. If the main intention of an article is to make a general (i.e. model independent) statement about the usefulness of a new development, but the usefulness is shown with the help of one specific model, the model name and version number must be stated in the title. The title could have a form such as, "Title outlining amazing generic
30   advance: a case study with Model XXX (version Y)".

R.1.3. Please see response to request above. IMOGEN v2.0 corresponds to the new calibration against a set of 22 GCMs. This paper is presenting a new model version.

35   C.1.4. All papers must include a section, at the end of the paper, entitled 'Code availability'. Here, either instructions for obtaining the code, or the reasons why the code is not available should be clearly stated. It is preferred for the code to be uploaded as a supplement or to be made available at a data repository with an associated DOI (digital object identifier) for the exact model version

described in the paper. Alternatively, for established models, there may be an existing means of accessing the code through a particular system. In this case, there must exist a means of permanently accessing the precise model version described in the paper. In some cases, authors may prefer to put models on their own website, or to act as a point of contact for obtaining the code. Given the impermanence of websites and email addresses, this is not encouraged, and authors should con- sider improving the availability with a more permanent arrangement. After the paper is accepted the model archive should be updated to include a link to the GMD paper.

R.1.4. The main basis for the paper is the new driving dataset – the patterns and EBM parameters forcing the IMOGEN model, rather than the model itself. However, these developments in available drivers are sufficiently large as to constitute a new model version - here named v2.0. The original model is written out in full in existing papers, including an earlier Huntingford et al 2010 GMD paper. Unfortunately our original paper version had the link to our archived model drivers named "Data Availability". This is now renamed "Data and Code Availability".

The driving dataset described in this paper was placed on a permanent and well-recognised international archive EIDC, and is now linked appropriately from the manuscript. In addition, we now also cite the 2010 GMD paper regarding the model description, and add: "For current IMOGEN code, please contact the corresponding author" (page 12, from line 26).

C.1.5. If I understood your article correctly, the main model you developed is IMOGEN, therefore a version number of IMOGEN should be given in the title and a code availability section should inform the reader about if and how to gain access to IMOGEN.

R.1.5. Agreed; and implemented as explained above, including within the title "IMOGEN vn2.0".

3

Response to gmd-2016-221-RC1 (Interactive comment from S. Emori - Referee)
Please note that some internal numbering from the review has changed slightly as review comments have been incorporated.

5

Comment 2.1. The paper describes a system for emulating CMIP3 climate models in terms of land surface variables at low computational cost, including its design, performance, applications and limitations. The manuscript is clearly written. I understand the importance of the attempt and usefulness of the tool, although honestly I felt that CMIP3 models are relatively dated and the authors might have been able to adopt CMIP5 data sooner. I have a couple of overall comments, which are rather my impression and not something really critical.

Response 2.1. We thank the referee for this review and a number of useful comments. We accept that a dataset based on the CMIP5 dataset is required. However, as we outline in the paper, a number of studies are based on the combination of the IMOGEN model and the presented set of patterns. This paper is intended to describe in a greater detail the dataset and how it was derived. We intend to work with an equivalent dataset based on CMIP5 and believe that there will be a benefit that we can refer back to the dataset described here, allowing comparison.

20 C.2.2. In my view, a climate emulator like the one presented here based on an energy balance model and pattern scaling is particularly powerful when it is applied for exploring a wide range of different scenarios (e.g., intermediate levels between RCPs). If the authors agree with this, it should be mentioned with more emphasis.

25 R.2.2. Agreed; we have already mentioned this briefly in the abstract, and in the beginning of the Introduction, but now we have expanded the later according to this suggestion (from line 9). In the Introduction, we now write:

"It allows interpolation away from a limited number of available GCM simulations, enabling a time-efficient assessment of surface meteorological changes for alternative non-standard future scenarios of changed GHG concentrations. This can include, for example, new scenarios that fall between the current Representative Concentration Pathways (RCP, Taylor et al., 2012), and potentially to investigate the current focus on targeting pre-defined future temperature thresholds such as two degrees"

35

C.2.3. The applications described are mostly focused on ecosystem impacts. I reckon however that the tool has a potential to be applied to a wider range of impact studies, including water resource, agriculture, health and so on. It could also be emphasized.

R.2.3. Agreed, and some of these potential applications we hope to pursue, so having IMOGEN v2.0 published will be helpful. Combining this comment with the suggestion from the Referee #2, we have added a new part to Section 4 "Applications" in which we undertake an assessment of IMOGEN performance in terms of ability to project changes to impacts, rather than just the direct climatic changes. We focus on mean annual total runoff, and making a direct comparison to GCM estimates of change. We also added a new figure (#7). Please see response 3.1 below.`

Minor comments:

C.2.4. P.2, L.2, "Global Climate Models (GCMs, also called Earth System Models, ESMs)": In my understanding, a GCM is called an ESM especially when (or only if) it incorporates some biogeochemical components. Simply paraphrasing them sounds uncomfortable to me.

R.2.4. Agreed. Following this suggestion, and the one from Referee #2 (3.1.), we have dropped the use of "Earth System Model" description in the case of the analysed CMIP3 data.

C.2.5. P.3, L.1, "Intergovernmental Panel for Climate Change": "on" instead of "for".

R.2.5. Corrected.

C.2.6. P.4, L.33, "50 km (e.g. MIROC3.2hires model,": The atmospheric resolution of MIROC3.2-hires is T106, which is approximately 100 km in mid-latitudes
instead of 50 km.

R.2.6. Corrected.

C.2.7. P.5, L.14, "climate regime c": Not clear what it means.

R.2.7. Changed to "climate regime in the decade c"

C.2.8. P.5, L.22, "one regression co-efficient, rather than two." Not entirely clear to me. Do you mean only slope rather than slope and intercept (or, equivalently, intercept is always zero)?

R.2.8. Yes, that is what we meant, and this is now stated more clearly in the same place. We now write: "This implies that the regression line starts at the origin of the coordinate system, so the intercept equals zero, and there is a fit with just one regression co-efficient, the slope"

5

C.2.9. P.5, L.33, "(ii) a constant ratio of mean land and ocean surface (SST) rate of warming, ν, (iii-iv) climate sensitivity over land λl and ocean λo (W m-2 K-1)": Instinctively, it sounds over-specification to me, as it looks like ν could be calculated by $\lambda l/\lambda o$ (at least approximately). It might be my silly misunderstanding, but a bit of further explanation might be helpful to other readers as well.

R.2.9. Whilst we agree that having individual climate sensitivities over land and ocean might initially seem an over-specification, the concern we had is that the ocean component of the global energy balance behaves very differently to the land surface. The ocean is a huge store of thermal energy, currently making the planet lag significantly - by decades - behind the true level of committed warming for current atmospheric GHG concentrations. Relative to the oceans, the land operates so as to have almost negligible thermal capacity, and hence we wanted to capture both effects individually. This also suggests thermal energy flows by atmospheric transport from the land regions to the oceans regions. Initially in Huntingford and Cox (2000), we tested this by modelling an advection term k*(dT_air-dT_ocean), but the fit was poor. Instead we found we could close the equations, capturing GCMs well, with simply a land/atmosphere fixed contrast. This gives an implicit advection, with "k" being a function of time. It is still an area of open research as to why both historical measurements and GCMs all project near-constant (in time) land/atmosphere contrasts.

C.2.10. P.6, L.13, Eq (2): "(is, ms, g)" in the r.h.s might have to be "(gs, ms, i)".

R.2.10. Agreed – thank you very much for spotting this mistake.

C.2.11. P.16, L.22: "Shiogama, H., Shiogama, H.,": duplicated. Please delete one.

R.2.11. Deleted

6

Response to gmd-2016-221-SC1 (Interactive comment from Anonymous Referee #2)
Please note that some internal numbering from the review has changed slightly as review comments have been incorporated.

Comment 3.1. As it stands, this paper is a simple implementation of the idea of pattern scaling and EMB calibration to a multi-model ensemble. I do not think any of this is new per se, and the choice of presenting this work based on a by now obsolete CMIP ensemble, CMIP3, does not help making the case for publication as is. That said, I think the value of the work resides in the provision of a multivariate set of fields/patterns, for the use in impact work, effectively exemplified by the motivating application through the IMOGEN system. This is in my opinion the real contribution of this work, but the focus of the paper is not adequately trained on this aspect. I would recommend major revisions, but I would hope that my request would not be a show stopper: what I would like to see is the application section expanded, not because I want to see the results of the impact analysis for their own value, but because I think we need to see how the pattern scaling performs in the application context, compared to results obtained from using the actual GCM output (by the way, I do think the use of ESM here is not appropriate, I don't think any of the CMIP3 models was an ESM in the sense of including a representation of the carbon cycle). My main concern is to be able to assess how the differential performance of the pattern scaling approach across variables and across models impacts the results of a multi-model impact assessment. I do not think the application section at this time addresses that.

Response 3.1. We thank the Referee for this constructive criticism. First, on notation and similar to the request of referee one, we have dropped the use of "Earth System Model" description in the case of the analysed CMIP3 data.

Based on this comment, we have expanded significantly Section 4 "Applications" in which we undertake an assessment of IMOGEN performance in terms of ability to project changes to impacts. The focus is placed on mean annual total runoff, and making a direct comparison to GCM estimates of change. We also added a new Figure 7. The new diagram, its caption and associated new text in main body of the paper is repeated below.
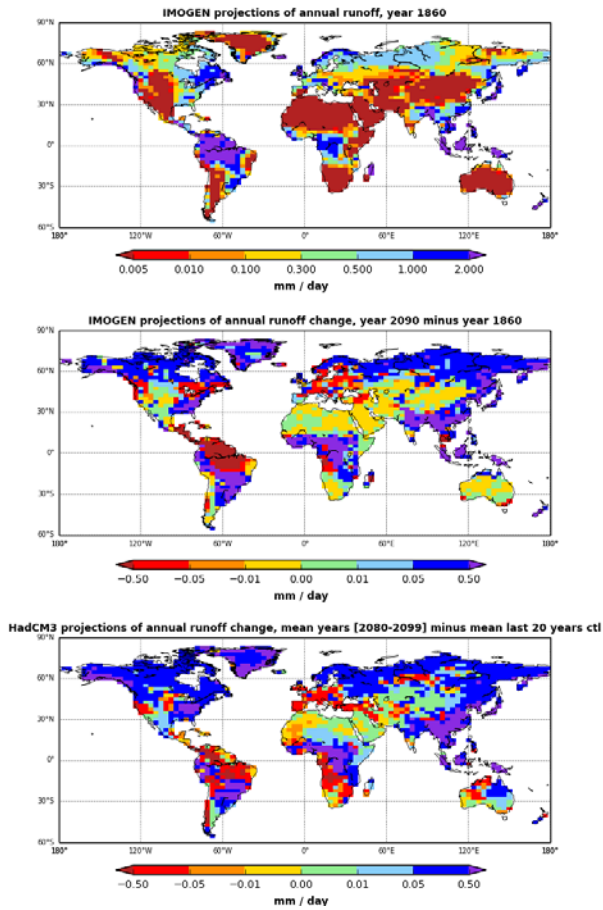
Figure 7 (Caption – figure below): Estimates of gridbox mean annual total runoff, RTot (mm/day). These are: top panel, for IMOGEN and year 1860: middle panel, IMOGEN estimates and year 2090 calculations of R_{Tot} minus those of year 1860: bottom panel, HadCM3 estimates and mean of year 2080-2099 calculations of R_{Tot} minus those of mean of last 20 years of pre-industrial control simulation.

New text: "We additionally undertake an assessment of IMOGEN performance in terms of ability to project changes to impacts, and when compared directly to GCM estimates of change. Many of the components of the land surface component of IMOGEN, i.e. JULES, remain similar to those operated in the HadCM3 GCM. Hence we evaluate an IMOGEN simulation operated with the HadCM3 patterns, by assessing performance against terrestrial diagnostics directly from the HadCM3 model. For both IMOGEN and HadCM3 simulations, this is with SRESA2 CO_2 emissions and estimated non-CO_2 radiative forcing also for that scenario, and with the GCM calculations drawn from the CMIP3 database. The variable we select is total runoff, which is the combination of surface and subsurface runoff calculations. This is available from both IMOGEN and HadCM3, and here presented as annual gridbox mean value, RTot (mm day^{-1}).

Runoff provides a challenge for comparison, as it is frequently a relatively small number between two larger fluxes of precipitation and evapotranspiration (transpiration, plus soil evaporation and interception loses) and so sensitive to change in those fluxes. Direct comparison also needs to account for IMOGEN being initialised with a climatology based on the CRU dataset, and temporal dis-aggregation to sub-daily drivers of JULES having not been calibrated against any particular GCM. Nevertheless, to be a useful tool for impacts assessment, then IMOGEN must capture the general features of GCM projections when operated for similar emissions scenarios.

In Figure 7, we compare IMOGEN versus HadCM3 projections of change in R_{Tot}. The top panel is modelled year 1860 values, from IMOGEN. The middle panel is the change in R_{Tot}, again for IMOGEN, and between years 1860 and 2090. The bottom panel is the change in R_{Tot} for HadCM3, comparing the last 20 years of the pre-industrial control simulation against the last 20 years of SRES-A2 forced simulation, which for the latter is 2080-2099. Multi-year averages are derived to remove any inter-annual variability, which as yet, IMOGEN does not represent. Although there are apparent local differences, and recognising the caveats above, then at its most general many dominant geographical features of change in IMOGEN do have similarities to those of HadCM3."

C.3.2. A particular concern is how the performance on individual variables translates into a performance across variables, i.e., in their joint behavior, for different models' output. In fact, in this regard, even the section about "Explanatory power of linear approximation" needs a better description: What is the meaning of the sentence (and I summarize) "Overall, climate patterns explain one third of regional climate change". How is the joint variability/covariability of the variables evaluated? Is the covariance patterns among all variables taken into account? I would like to see

9

a more rigorous and formal definition of how the variance of the joint set of variables is represented by the emulation.

R.3.2. We agree that the issue of co-variability is important, and are aware of the studies that look in to more complex pattern-scaling models which partly address this issue (e.g. Frieler et al 2012, now cited in this manuscript). We request, that on this one issue, this is beyond the scope of this presentation of the IMOGEN 2.0 model.

However we do acknowledge some poor wording in the paper. First, the section of concern is now titled: "**3.3. Performance of linear approximation assumption in "pattern-scaling" for individual variables".**

Then, in that Section, we now write more clearly, adding "when per-variables results are averaged" as: "Overall (i.e. when per-variable results are averaged, without considering co-variance), climate patterns explain one-third of regional climate change (PVE 34.25±5.21)"

C.3.3. If the authors are willing to show how the use of the pattern scaling solution compares to the use of the original output from the multi-model ensemble I think the article will become more informative and valuable to the impact research community, within and beyond IMOGEN users. In this respect I also agree with Dr. Emori that the potential is larger than just the IMOGEN application and it would be good to point that out.

R.3.3. We agree, and have expanded extensively our Section 4 "Applications", with a focus on change in mean annual total runoff. This is by a direct comparison between GCM estimates of change (for HadCM3), and IMOGEN estimates. Please see our response to query C.3.1. above, including listing of new diagram, caption and additional text within the manuscript.

C.3.4. Last, two very minor points: I think throughout the paper the word "assembly" has been erroneously substituted for "ensemble", my guess because of an auto-correct program.

R.3.4. Corrected – thank you very much for noticing this mistake.

C.3.5. The other word, which I think is used instead deliberately but I question, is "meteorology". I think what the pattern scaling approach produces is still "climatology". These are after all ten-year means. The use of a weather generator may then produce meteorology at the time scale needed by the impact model, but that is an add-on to the method that this paper focuses on.

R.3.5. We agree that "climatology" is more accurate and would like to explain that originally we referred to "meteorology" because of IMOGEN`s weather generator. Six instances of "meteorology" have been changed throughout the text to "climatology".

5

Climate pattern scaling set for an ensemble of 22 GCMs – adding uncertainty to the IMOGEN vn 2.0 impacts system

Przemyslaw Zelazowski[1,2], Chris Huntingford[3], Lina M Mercado[4,3] and Nathalie Schaller[1,5]

[1]Oxford University Centre for the Environment, University of Oxford, Oxford, OX1 3QY, UK

10   [2]Centre of New Technologies, University of Warsaw, Warsaw, 02-097, Poland

[3]Centre for Ecology and Hydrology, Wallingford, OX10 8BB, UK

[4]Geography, College of Life and Environmental Sciences, University of Exeter, Exeter, EX4 4RJ, UK

[5]Center for International Climate and Environmental Research (CICERO), Oslo, NO-0318, Norway

Correspondence to: Chris Huntingford (chg@ceh.ac.uk)

15   **Abstract.** Global Circulation Models (GCMs) are the best tool to understand climate change, as they attempt to represent all the important Earth system processes, and including anthropogenic perturbation through fossil fuel burning. However, GCMs are computationally very expensive, which limits the number of simulations that can be made. Pattern-scaling is an emulation technique that takes advantage of the fact that local and seasonal changes in surface climate are often approximately linear in amount of warming over land and globe. This

20   allows interpolation away from a limited number of available GCM simulations, to assess alternative future emissions scenarios. In this paper we present a pattern-scaling set consisting of spatial climate change patterns along with parameters for an energy balance model that calculates the amount of global warming. The set is derived from 22 GCMs of the WCRP CMIP3 database, setting the basis for similar eventual pattern development for CMIP5 ensemble. Critically, it extends the use of the IMOGEN (Integrated Model Of Global Effects of climatic

25   aNomalies) framework to enable scanning across full uncertainty in GCMs for impacts studies. Across models, the presented climate patterns represent consistent global mean trends, with maximum four GCMs exhibiting opposite sign of the trend per variable (relative humidity). The described new climate regimes are generally warmer, wetter (but with less snowfall), cloudier and windier, and with decreased relative humidity. Overall, when averaging individual performance across all variables, and without considering co-variance, the patterns

30   explain one-third of regional change in decadal averages (mean Percentage Variance Explained, PVE, 34.25±5.21), but signal in some models exhibits much more linearity (e.g. MIROC3.2(hires):41.53) than in others (GISS_ER: 22.67). The two most often considered variables: near-surface temperature and precipitation, have

11

Deleted: (i.e.

Deleted: per-variable

Deleted: results are averaged,

Deleted:)

Deleted: of the analysed variables

PVE of 85.44±4.37 and 14.98±4.61, respectively. The dataset is available for download and researchers in the areas of ecosystem modelling and climate change impact assessment are already starting to use it. Besides allowing time-efficient assessment for non-standard future scenarios of changed greenhouse gas (GHG) concentrations, it enables understanding of new representations of land surface processes, and including climate-carbon cycle feedbacks. Current and potential future applications of such modelling system are discussed.

1 Introduction

Global Climate Models (GCMs) are the primary source of our understanding of and ability to estimate future climate regimes resulting from anthropogenic Greenhouse Gas emissions (GHGs). However, the use of these tools is limited by their requirements for computing power, and the complexity of the task, in particular in the case of multi-model assessments. "Pattern-scaling" (Huntingford & Cox 2000, Mitchell et al 2003), is a methodology that takes advantage of the fact that, to a reasonable approximation, local and seasonal changes in surface climate are linear in amount of warming over land and globe. It allows interpolation away from a limited number of available GCM simulations, enabling a time-efficient assessment of surface meteorological changes for alternative non-standard future scenarios of changed GHG concentrations. This can include, for example, new scenarios that fall between the current Representative Concentration Pathways (RCP, Taylor et al., 2012), and potentially to investigate pre-defined future temperature thresholds such as two degrees.

"Climate-change patterns" (or "patterns") are coefficients of the regression between mean warming over Earth's land regions, ΔT_l (K) and local changes in surface climatology. They are derived by comparison against outputs from GCMs, and presented as local monthly mean changes over land per degree of mean global over land. "Pattern-scaling" is a simple procedure in which these patterns are multiplied by ΔT_l to give local changes in climatology. A global Energy Balance Model (EBM; e.g. Wigley et al. 2000) is then applied to model how the GHG concentrations translate into changes in radiative forcing, Q (Wm^{-2}) and then into temperature increase over land regions (ΔT_l).

The IMOGEN framework (Integrated Model Of Global Effects of climatic aNomalies; Huntingford et al. 2010) is a computationally efficient tool for modelling impacts of future climate change on terrestrial ecosystems. It consists of the JULES land surface model (Best et al., 2011; Clark et al., 2011) linked to a pattern-scaling module (Huntingford and Cox, 2000). The scaling provides monthly mean changes in climate variables over land, notably temperature, relative humidity, precipitation and radiation - quantities used to drive ecosystem models. In addition, a simple oceanic global carbon cycle model is included (Joos et al., 1996 and Appendix of Huntingford et al., 2004), which expands the typical usage of patterns-scaling by allowing consideration of oceanic climate-carbon cycle feedbacks, alongside land-based feedbacks. All simulations use an hourly time step and a spatial resolution of 2.5° latitudinal x 3.75° longitudinal, or 72 by 96 grid boxes, as in the UKMO-HadCM3 GCM. Over land, but excluding Antarctica, this corresponds to 1631 grid-boxes. Linking forcings to mean warming over land, ΔT_l, is achieved with the EBM which requires five parameters, described in the Methods section. The relevant equations are presented in Huntingford and Cox (2000). The five parameters are referred to as IMOGEN EBM

12

Deleted: , also called Earth System Models, ESMs

Deleted: ,

Deleted: intermediate levels

Deleted: if more relevant to the considered scenario

Deleted: the current focus on targeting

Deleted: meteorology

Deleted: meteorology

Deleted: a

Deleted:

Moved down [1]: All the energy retained in the planetary system, and as seen in any difference in top-of-the-atmosphere radiation, is assumed to enter the oceans in a diffusive process, and thus changing SSTs and then ΔT_l via v.

calibration parameters (or simply "calibration parameters"), and, as in the case of patterns, they are also derived from GCM runs. The "patterns" and "calibration parameters" together form a "patterns-scaling set".

IMOGEN was originally established to allow rapid assessment of a range of alternative GHG emission scenarios, e.g. corresponding to the standard Special Report on Emissions Scenarios, (SRES, Nakićenović et al, 2000) or
5 Representative Concentration Pathways (RCP, Taylor et al., 2012) where GCM simulations are unavailable, as well as interpolating away from what GCM simulations do exist to new user-prescribed emissions or concentration pathways. RCPs were used to inform the recent 5th IPCC report (IPCC, 2013), via the set of climate model simulations available at that time in the CMIP5 dataset (Taylor et al 2012). CMIP5 has evolved further since year 2013 and to hold more simulations; the exercise to calibrate a patterns-scaling set for CMIP5 is under
10 way. Normally, evolving atmospheric carbon dioxide (CO_2) concentrations are calculated as a consequence of prescribed CO_2 emissions, along with prescription of non-CO_2 forcings for other GHGs and aerosols. Then an overall radiative forcing Q is calculated to drive the EBM. Alternatively, all radiative forcing Q can be prescribed directly as future forcings' pathways, in which case CO_2 concentrations are prescribed, again for scenarios that differ from the standard ones.

15 In practise, though, IMOGEN has been used more to assess the effects of new parameterisations, adjustment or inclusion of new processes into the land surface model. This is as a precursor for any eventual inclusion of land surface model improvements in a full GCM. IMOGEN allows easy and fast assessment of ranges of parameterisations, numerical stability checks and critically the relative importance of new understanding of ecological and hydrological responses globally, and including feedbacks on the carbon cycle. Examples include
20 the impacts of changes in diffuse radiation on the land carbon sink (Mercado et al., 2009), or the effects of ozone damage on plant productivity (Sitch et al 2007).

Until recently, these offline studies were performed with patterns of climate change from a single model, UKMO-HadCM3 (IMOGEN version 1.0, Huntingford et al., 2010). The purpose of this paper is to present a patterns-scaling set which emulates a broad range of GCMs, and nearly the complete set of those held in the
25 WCRP CMIP3 database (Meehl et al., 2007). This extends the use of IMOGEN for assessment of climate change, or land surface response, to scan across uncertainty in climate models. Such uncertainty can then be evaluated against any further uncertainty in any terrestrial surface impacts of interest. In Section 2 we describe the methods which lead to the patterns-scaling set. Section 3 describes the actual set, including discussion of found inter-GCM differences, and we include metrics describing the accuracy of the linearity assumption of
30 meteorological changes against level of global warming, as implicit in the scaling method. Section 4 reviews existing applications of the IMOGEN pattern-scaling system and comments on the future benefits of inclusion of our climate model uncertainty. Finally, Section 5 discusses the strengths and caveats of the pattern-scaling approach.

2. Data and Methods

2.1 The WCRP CMIP3 multi-model dataset and data pre-processing

Spatial patterns (i.e. maps) of climate change and energy balance model calibration parameters (together forming the "climate-patterns set") are derived from GCM data available through the World Climate Research Programme Coupled Model Intercomparison Project, phase three (WCRP CMIP3; Meehl et al., 2007). The WCRP CMIP3 multi-model dataset resulted from an international effort to run a coordinated set of twentieth- and twenty-first-century climate GCM simulations for a small prescribed number of future scenarios, covering many aspects of climate variability and change. All these simulations were subsequently analysed and formed the basis of much that is reported in the Fourth Assessment (AR4) of the Intergovernmental Panel on Climate Change (IPCC, 2007). The dataset consists of data from 24 GCMs, representing 17 modelling groups from 12 countries. The climate patterns set presented here (Table 1) corresponds to 22 GCMs, because GISS_AOM is an atmosphere-ocean model without surface meteorological projections over land and key data from CGCM3.1(T63) GCM were missing (see below). In the case of GISS-EH and GISS-ER GCM, WCRP CMIP3 data were supplemented with the formally associated pool provided by National Aeronautics and Space Administration Goddard Institute for Space Studies (http://data.giss.nasa.gov/pub/pcmdi).

The analysed model runs represent scenarios of four types: (i) control experiments: either pre-industrial or present day (Picntrl, or Pdcntrl), (ii) the idealized 1% yr^{-1} CO_2 increase up to doubled and quadrupled levels (1pctto2x, 1pctto4x), (iii) the twentieth-century run (20C3M) representing modelled period from pre-industrial to present-day and (iv) the high- (A2) and mid-emission (A1B) future scenarios defined by the Special Report on Emission Scenarios (SRES, Nakicenovic et al. 2000). When multiple simulations are available of any particular scenario, then the analysis is limited to the first available, as the inter-run variability has been reported to be small (Frieler et al 2012).

Variables analysed for each GCM are those representing land surface climatology: 1.5 m air temperature (TAS), 1.5 m relative humidity (HURS), 10 m wind speed (UAS and VAS, combined into direction-less UA), precipitation (PR, including snow PRSN), downward shortwave (RSDS) and long-wave (RLDS) radiation fluxes and surface pressure (PS). The codes in brackets are the name conventions used in the WCRP database for individual variables. It is these variables that are required to run the JULES land surface scheme inside the IMOGEN framework. Additionally, Net Radiative Flux at the top of the atmosphere (positive downwards); Top of Model (RTMT); is also processed, as this is required to drive the global energy balance model.

There were some discrepancies between data requirements to run the IMOGEN system and the actual data availability in WCRP CMIP3. They are listed in Table 1. For all GCMs, surface relative humidity (HURS) data was not available, but a 4D representation of this variable at pre-defined pressure levels (HUR) was generally available. This allowed extrapolation of surface relative humidity from two highest available pressure levels which are near the land surface. In the case of INGV-SXG, PCM and CCSM3 GCMs, surface wind was obtained in the same procedure. For two cases, the required surface data was available, but suffered from quality and other issues. In UKMO-HadGEM1 data, last month of the SRES A2 simulation was missing (and in this study it was

| Deleted: for |
| Deleted: 1 |
| Deleted: meteor |

filled-in with interpolated values), and surface wind data was presented on non-standard grid (and it was interpolated onto a standard UKMO-HadGEM1 grid). For MRI-CGCM2.3.2, many values in snow precipitation data (PRSN) were missing (the data were not used in this study) and there was no land mask available (SFTLF, later obtained from the Japanese modelling group). Finally, in the case of four GCMs certain non-critical

5   variables were entirely missing (Table 1).

GCMs differ significantly between each other in the spatial grid resolution and generally how they represent the Earth surface's detail (as represented in the "land mask" variable SFTLF which reports gridbox land fraction). Spatial resolution varies between hundreds of kilometres (e.g. GISS models, or INM-CM3.0) to c. 100 km (e.g. MIROC3.2hires model, mid-latitudes, Table 1). Data are mapped on either a regular or a Gaussian grid, and

10   gridbox classification into land and water is either binary (either 100% or 0%) or continuous, with only a part of GCMs explicitly depicting freshwater bodies in their land masks. This diversity of output spatial properties alone imposes a challenge for data end-users, including policymakers, especially when it comes to multi-model assessments of a pre-defined geographical domain. To force our common land surface model within the IMOGEN system using alternative GCM-based estimates of climate change, we harmonised all types of WCRP

15   CMIP3 grids into one, which was chosen to be the UKMO-HadCM3. This ensures compatibility with previous applications of the IMOGEN tool, with resolution of 2.5° latitudinal x 3.75° longitudinal. The common grid allows, in a systematic way, to capture the impact of climate uncertainty that remains within GCMs. More information about this re-gridding procedure is provided in the Supplementary Material.

2.2 Climate pattern scaling set and post-processing

20   The presented climate patterns are a set of regression coefficients, each representing the change per degree of mean global warming over land, while the fitting is done with decadal average changes against the global mean warming over land, as predicted by each GCM. The simple form of the analogue model for an anomaly (Δ) in one of the considered land surface variables V in the climate regime in the decade c can be described as:

$$\Delta V(c, g, m, i) = \Delta T_l(c, i) V_x(g, m, i) \hspace{3cm} (1)$$

25   where the anomaly is linked to a single location on the UKMO-HadCM3 grid (g), month of the annual cycle (m), GCM (i) and decadal time index (c). Regressions to find patterns V_x use global land warmings ΔT_l directly from original GCMs, but when the IMOGEN model is used predictively, then these values are derived using an Energy Balance Model (EBM) component (see below).

Regressing local climate with mean land warming is done with the assumption that climate is stable before the

30   anthropogenic impact. This implies that the regression line starts at the origin of the coordinate system, so the intercept equals zero, and there is a fit with just one regression co-efficient, the slope. This starting point is represented by an average of three decades from the twentieth-century run (20C3M, years 1961-1990, Figure 1, panel C) which is a period corresponding to the Climate Research Unit's Time Series 2.1 (CRU TS 2.1) dataset describing Earth's climatology (or "climate normals", Mitchell and Jones 2005). In the WCRP CMIP3 dataset, the

35   historical 20C3M GCM simulations are normally followed by a future transient run, driven by one of SRES scenarios that describe potential pathways ahead in emissions. In the presented work, for most of GCMs, a

15

high-emissions "business-as-usual" SRES A2 run was analysed, while in a few cases when these data were not available the SRES A1B run was used (Table 2), which represents relatively lower levels of warming (Nakicenovic et al. 2000).

Emulating an ensemble of GCMs requires that the relationship between anthropogenic climate forcings, global warming and warming over land is established for each GCM separately. The EBM, described in full in Huntingford and Cox (2000), requires the fitting of five calibration parameters to a simple global energy balance model: (i) an ocean effective thermal diffusivity, κ (Wm^{-1}K^{-1}), (ii) a constant ratio of mean land and ocean surface (SST) rate of warming, v, (iii-iv) climate sensitivity over land λ_l and ocean λ_o (W m^{-2} K^{-1}), and (v) land fraction f (variable SFTLF, including Antarctica). All the energy retained in the planetary system, and as seen in any difference in top-of-the-atmosphere radiation, is assumed to enter the oceans in a diffusive process, and thus changing SSTs and then ΔT_l via v. Estimation of EBM parameters was done by fitting them against an independent set of scenarios: the idealised CO_2 increase scenario (1pctto2x or 1pctto4x), preceded by a control experiment: (Picntrl or Pdcntrl). Subsequently, functioning of the parameterised EBM was validated – that is, it was used predictively - against data from one of the available runs corresponding to SRES scenarios (SRES A2 or SRES A1B, Table 2). Figure 1 illustrates the key components of the process of deriving a pattern-scaling set in the case of the UKMO-HadGEM1 GCM.

In general, our climate patterns represent absolute changes. However, for precipitation, we make one additional calculation which results in data normalisation. This is to circumvent the problem of particularly large biases in the description of the current precipitation regime by some GCMs (Ines and Hansen 2006). For each calculated precipitation pattern (ΔP), this is then multiplied by the ratio of the observed precipitation (P_{CRU_XXc}) from the CRU TS 2.1 dataset (Mitchell and Jones 2005) and the one simulated by the GCM (P_{GCM_XXc}) for the control period. This follows Ines and Hansen (2006), and Malhi et al. (2009):

$$\Delta P'(g,m,i) = \Delta P(g,m,i) \times \frac{P_{CRU_{XXc}}(i,m_S,g_S)}{P_{GCM_{XXc}}(i,m_S,g_S)} \qquad (2)$$

Furthermore, the adjustment of Eqn. (2) was performed for each grid box g, month m and GCM i, after smoothing in time and space (averaging over the grid box and its immediate neighbourhood: g_S, and across three months m_S). This reduce significantly the number of artefacts caused by occasional division by near 0. The remaining few cases of high and low divergence (i.e. $P_{CRU,XXc}/P_{GCM,XXc}$) were capped at 5 and 0.2. Snow was scaled according to the same scaling factor as total precipitation. The final patterns set is available in two versions: with precipitation normalised by Eqn. (2), and without this.

As a last step, in four cases when available GCMs data had one or two non-key variables missing (Table 1), the gaps were filled in with across-ensemble means.

16

3 Results

3.1 Energy balance parameters

The five key EBM parameters are presented in Table 2. In most cases (17) climate sensitivity over ocean (λ_o, $Wm^{-2}K^{-1}$) is higher than over the land (λ_l, $Wm^{-2}K^{-1}$). The reverse trend is well pronounced in three models (CSIRO-
5 Mk3.5, MIROC3.2highres, MRI-CGCM2.3.2). Climate sensitivity over land varies five-fold between models and is the lowest in ECHO-G, UKMO-HadCM3, CGCM3.1(T47) and the highest in BCCR-BCM2.0, PCM, FGOALS-g1.0, although 2/3rds of the models have a much narrower range 0.9-1.7 $Wm^{-2}K^{-1}$. The most varying variable is ocean diffusivity (κ, $Wm^{-1}K^{-1}$), which determines the ability of the ocean to extract heat from the climate system through diffusion. Even after excluding the two most extreme cases, the range remains high: from 270
10 (HadCM3, CGCM3.1(T47)) to 2800 $Wm^{-1}K^{-1}$ (CSIRO-Mk3.0). The most extreme value of 11000 $Wm^{-1}K^{-1}$ is for the FGOALS-g1.0 GCM, which clearly stands out from the ensemble. This spread reflects the fact that a full understanding of oceanic flows and deeper overturning, which affects mean vertical heat transport, is still required to reduce model spread. In comparison, the land/ocean temperature increase contrast (v) is a remarkably stable parameter, with a range 1.40-1.78 across all models.

15 ## 3.2. Patterns across models, space and seasons

Across models, patterns of particular variables represent consistent trends when averaged spatially and across months (Table 3), with maximum four exceptions per variable (relative humidity), i.e. cases when average pattern is of opposite sign than in the majority of GCMs. The patterns capture the nature of a new emerging climate regimes, which can be characterised as warmer, wetter (but with less snowfall), cloudier and windier,
20 with decreased relative humidity, and increased atmospheric pressure. Globally, relative humidity stands out as the variable with the highest uncertainty in the magnitude of change, with SD across the models exceeding the mean. In the case of other variables apart from longwave downward radiation and air temperature near surface (RLDS, TAS, with very small spread) the magnitude of standard deviation is similar (62-88 % of the mean).

In the case of each GCM, the patterns represent a unique regional and seasonal distribution of change in
25 surface climatology in a greenhouse-gas enriched atmosphere. To present these differences, we focus on two of the strongest drivers of terrestrial ecosystems change (and co-incidentally, which are also having the largest influence on society in general) – that is adjustments to temperature and precipitation. The annual mean rate of warming per degree of global warming over land (Figure 2) in some models is much more evenly distributed geographically (e.g. BCCR-BCM2.0) than in others (e.g. NCAR-PCM1). However, all of the models exhibit the
30 majority of warming in Northern latitudes. The smallest warming occurs in tropical Africa and Asia, while in tropical South America the magnitude is much more uncertain. The spatial pattern of warming is either well stratified with latitude (e.g. FGOALS-g1.0 model), or more nuanced (GISS models). The patterns of precipitation change (Figure 3) are more complex and in some regions they exceed the uncertainty in regional warming (e.g. South America); however, in other areas the signal is very consistent, such as drying of Southern Europe.

35 Across-model seasonal averages (Figure 4 and 5, for temperature and precipitation respectively) reveal a more spatially and temporally consistent picture than when considering models individually. These figures show that

17

Deleted: assembly

Deleted: climate

Deleted: meteor

the majority of warming occurs on Northern latitudes during colder seasons. Moreover, there is a strong summer warming trend over mid-West North America, Mediterranean region, Middle East and Central Asia. The seasonal patterns of precipitation change appear as linked to those of temperature, but are generally more uncertain. Winter warming in the North is accompanied by more precipitation which contrasts with lower

5   summer warming and reduced rainfall. Changes in tropical rainfall appear as much more uncertain. Western and Central Africa north of equator is a zone with particularly high uncertainty regarding summer warming.

Stippling in Figure 5 provides additional measure of uncertainty - it indicates when there is agreement in 90% of the models, as to whether precipitation is going to increase or decrease. This is the case over most of the land area and seasons. However, in many dry areas and seasons where this measure is not robust due to low

10   precipitation levels (and the signal is difficult to detect), the agreement is uncertain. Some areas stand out in this regard: large parts of South America in northern winter and summer, high northern latitudes in the summer and central Asia in autumn. That rainfall changes remain a large uncertainty in climate model projections is noted in the 4th IPCC report (IPCC 2007).

3.3. Performance of linear approximation assumption in "pattern-scaling" for individual

15   variables

The robustness of climate patterns is assessed by their ability to reproduce the decadal GCM data. It varies widely between variables, which can be split into four categories, according to the mean Percentage Variance Explained (PVE) metric (Table 3), a simple way to assess each variable separately through the analysis of decadal means against the pattern. The most robust are the patterns which represent the drivers of global warming:

20   temperature TAS and long-wave radiation RLDS (PVE 85.44±4.37, and 84.74±4.97, respectively). The next group consists of variables, which explain around one quarter of variance: short-wave radiation RSDS and air pressure PS. Variables linked to availability of water: precipitation PR, snowfall PRSN, relative humidity HURS, form the third group (PVE 14.98±4.61, 17.96±4.67, 16.92±5.71, respectively). The last category is represented by wind patterns (of combined variables UAS and VAS), which represent only 7.11±3.32 PVE. Wind patterns also contain

25   the highest proportion of negative PVE (4.9%).

Overall (i.e. when per-variable results are averaged, without considering co-variance), climate patterns explain one-third of regional climate change (PVE 34.25±5.21); however, signal in some models exhibits much more linearity (e.g. MIROC3.2(hires): 41.53) than in others (GISS_ER: 22.67). These estimates exclude cases where the PVE statistic could not be calculated due to either a lack of data (2.8%, Table 1), or null (e.g. short-wave

30   radiation during polar night) and extremely low values (e.g. precipitation in the dry season), accounting for 6.7% of cases.

In terms of spatial distribution of robustness of the two key variables: temperature and precipitation (Figure 6), it is generally the opposite. For temperature, lower PVE values occur in the North, with minimum over Greenland and North-West North America (but still above 50%). The highest values occur across the Tropics. In

35   the case of precipitation, the highest PVE occurs over the northern latitudes (above 50°N), particularly in Asia. In some Tropical areas (sub-saharan Africa, South-East Amazon) areas with relatively robust signal (PVE ~20%) are

Deleted: North

Deleted: Equator

Deleted:

Deleted: Explanatory power

Deleted: of the analysed variables

Deleted: ,

Deleted: but s

adjacent to regions where the robustness could not be estimated due to very small and erratic rainfall in the dry season.

4. Applications

The "pattern-scaling" concept was originally designed as a tool for scientists to inform policymakers, enabling investigation of expected changes in surface climatology for a broader range of scenarios of atmospheric greenhouse gas concentrations than available in archived GCM runs. The original version of a framework capturing, in effect an interpolation methodology, was based around UKMO-HadCM3 GCM (Huntingford and Cox, 2000). Once the IMOGEN system (Huntingford et al., 2010) linked such scaling of meteorological drivers to force directly a land surface model, the main application of such framework has been to undertake global analyses of ecosystem response in a changing climate. Particular examples include quantification of wetland methane feedbacks (Gedney et al., 2004), the impacts of changes in diffuse radiation to the land carbon sink (Mercado et al., 2009), the effects of tropospheric ozone on plant productivity (Sitch et al., 2007), the significance of energy crop planting on future atmospheric CO_2 concentration (Hughes et al., 2010) and how alternative mixtures of changes in atmospheric composition, even corresponding to identical radiative forcing changes, can have very contrasting impacts on land surface carbon stocks (Huntingford et al., 2011).

The potential for Amazon forest collapse, or "die-back", remains an iconic concern for potential climate change impacts. Such a possibility has been identified in a combined climate-carbon cycle climate model UKMO-HadCM3LC (Cox et al 2000, 2004). Later, the robustness of predictions of Amazon 'dieback' were investigated with IMOGEN (version 1.0) and the original UKMO-HadCM3 patterns (Huntingford et al. 2008), by analysing the vegetation response to (i) some limited uncertainty via prescribed bounds in the parameterisations of the atmospheric component of UKMO-HadCM3 (related to HadCM3LC), (ii) description of canopy radiation interception – "big leaf" versus "multilayer" and (iii) representation of vegetation dynamics using an area based model and an individual based model. All simulations show a fairly robust dieback. More recently, a set of the climate patterns described in this paper were used to analyse the potential for tropical rainforest "die back". Zelazowski et al. (2011) combined the patterns and global contemporary climatology to produce high resolution maps of the future extent of humid tropical forests, while Huntingford et al. (2013b) forced the IMOGEN framework with the full set of patterns. Both studies found that models other than UKMO-HadCM3 are less likely to project such losses, which reflects the particularly stronger climatic signal for the Amazon region temperature and precipitation changes for UKMO-HadCM3, as noted in Figures 2 and 3 above.

In order to exemplify the ability of IMOGEN to project changes to impacts, we report results of the mean annual total runoff (R_{tot}, mm day^{-1}) simulation (Figure 7), and compare them directly to GCM estimates of change. Many of the components of the land surface component of IMOGEN, i.e. JULES, remain similar to those operated in the HadCM3 GCM. Hence we evaluate an IMOGEN simulation operated with the HadCM3 patterns, by assessing performance against terrestrial diagnostics directly from the HadCM3 model. For both IMOGEN and HadCM3 simulations, this is with SRESA2 CO_2 emissions and estimated non-CO_2 radiative forcing also for

19

that scenario, and with the GCM calculations drawn from the WCRP CMIP3 database. The variable we select is total runoff, which is the combination of surface and subsurface runoff calculations. This is available from both IMOGEN and HadCM3, and here presented as annual gridbox mean value, R_{tot}.

Runoff provides a challenge for comparison, as it is frequently a relatively small number between two larger
5 fluxes of precipitation and evapotranspiration (transpiration, plus soil evaporation and interception loses) and so sensitive to change in those fluxes. Direct comparison also needs to account for IMOGEN being initialised with a climatology based on the CRU dataset, and temporal dis-aggregation to sub-daily drivers of JULES having not been calibrated against any particular GCM. Nevertheless, to be a useful tool for impacts assessment, then IMOGEN must capture the general features of GCM projections when operated for similar emissions scenarios.

10 In Figure 7, we compare IMOGEN versus HadCM3 projections of change in R_{tot}. The top panel shows modelled year 1860 values, from IMOGEN. The middle panel shows the change in R_{tot}, again for IMOGEN, and between years 1860 and 2090. The bottom panel shows the change in R_{tot} for HadCM3, comparing the last 20 years of the pre-industrial control simulation against the last 20 years of SRES-A2 forced simulation, which for the latter is 2080-2099. Multi-year averages are derived to remove any inter-annual variability, which as yet, IMOGEN
15 does not represent. Although there are apparent local differences, and recognising the caveats above, then at its most general many dominant geographical features of change in IMOGEN do have similarities to those of HadCM3.

Whilst IMOGEN framework allows testing hypotheses in more advanced land surface configurations, such as JULES (Mercado et al., 2007), the major advantage of routine utilisation of the full set of patterns described in
20 this paper is that any assessment of uncertainty in how the land surface may function, for different levels of atmospheric greenhouse gases, can be now understood in the context of the full spectrum of uncertainty implicit in climate models from different GCM research centres. To aid this even further, ultimately the analysis of Sitch et al. (2008), in which the IMOGEN system is used to diagnose uncertainty in representation of future plant biogeography and climate-carbon cycle feedbacks using five Dynamical Global Vegetation Models
25 (DGVMs), but combined with only a single set of climate models patterns based on UKMO-HadCM3, can be re-visited. If each DGVM modelling centre could operate their latest DGVM configuration, across the range of emulated GCMs, then this would give a fuller estimate of the balance between implications of uncertainty in climate and uncertainty in terrestrial ecosystem response and its feedbacks on the global carbon cycle.

In some regards, land surface models in GCMs are still in their infancy, considering the growing knowledge of
30 how vegetation responds physiologically to imposed climatic changes. For this reason, there are many future plans to use IMOGEN as an intermediate step, before inclusion in a full GCM, to test and demonstrate the relative importance of a particular new understanding. For example, we have used the patterns derived on this paper on an analysis of the sensitivity of the future land carbon storage to thermal acclimation of plant photosynthesis (Mercado et al., in preparation). This is a noted major deficiency in current large-scale terrestrial
35 models (Booth et al 2012; Huntingford et al., 2013a; Smith and Dukes 2013). In addition, the assessment of newly available enhanced description of leaf dark respiration (Atkin et al., 2015) is needed, as well as the inclusion of both Nitrogen and Phosphorus constraints to plant productivity in tropical ecosystems (e.g.

Mercado et al., 2011), and inclusion of a full representation of a coupled Carbon-Nitrogen cycle in JULES (Zaehle et al 2010). Furthermore, it is desirable to test the effects of adding height competition into the vegetation dynamics module of JULES, in order to add ecological succession modelling (Smith et al 2001; Moorecroft et al 2001), along with assessing the impacts of improved representation of stomatal conductance (Medlyn et al 2011; Kala et al 2015) and plant hydraulics (Sperry et al. 2015) on simulated land carbon- and water-cycles to climate. The later could extend as far as testing any hormonal signalling in the hydraulic linkages between soil moisture and stomata response; an effect well known by the physiological community but hereto never tested in a full large-scale gridded land surface model (Huntingford et al., 2015). Finally, impacts of introducing a better representation of plant functional types and plant trait variation across space and time (Verheijen et al 2015) on simulated land carbon should also be considered.

5. Discussion

In this paper we present a "pattern scaling set", consisting of spatially explicit climate change patterns and EBM calibration parameters, which together represent 22 GCMs of the WCRP CMIP3 database (Meehl et al., 2007). This data set extends the use of the IMOGEN climate impacts assessment tool to scan across uncertainty in climate models. Despite relying on a set of simple assumptions, the tool can capture a significant part of the predicted changes in surface climatology. Terrestrial ecosystem response studies can use this modelling framework to gain new insights into how the land surface component of the Earth system functions.

An important aspect of the presented work is the comprehensive study of pattern's robustness, i.e. their ability to capture variability of climate simulated by GCMs. The fact that together the set of considered variables capture 1/3rd of decadal variability in monthly averages, suggests that it is a technique with a significant potential, especially since it allows a large reduction in input data and computation requirements through removal of the time dimension. Overall, the presented patterns are in good agreement with the results presented in the Fourth Assessment Report of the Intergovernmental Panel on Climate Change (see SI and Figure 10.9 in Meehl et al., 2007). This applies to both the multi-model mean changes in surface climate, as well as the degree of agreement between the models (stippling in Figure S3).

However, the ability of climate patterns to capture the course of changes varies significantly between the modelled climate variables. In contrast to temperature change (85.44±4.37% of variability explained by climate patterns), change in precipitation, which is amongst critical aspects of climate change, is generally relatively difficult to capture in this linear methodology. Into a large extent this is a consequence of the fact that the original GCM results are also relatively inconsistent as regards precipitation. In climate patterns this uncertainty is further exacerbated, and in consequence overall 85% of variability remains unexplained, although it should be noted that in some regions seasonal precipitation patterns explain up to 75% of variability (generally at high northern latitudes). The very poor performance in precipitation estimation over dry zones is in part because it is not possible to capture the trend through what are very low precipitation levels. In these areas, the mean change over decades gives low PVE values, as any change in very small current absolute precipitation can result

21

Deleted: meteor

Deleted: for

in high relative deviations from preindustrial levels. In such circumstances, precipitation is very much dominated by inter-annual fluctuations which mean scaling cannot be captured well.

The presented work is an attempt to unify the spatially heterogeneous GCM data resource. Placing on a common grid brings strong benefits to the IMOGEN tool. However as a result of the applied procedure for re-
5 gridding combined with land mapping (see Supplementary Material), the calculated regional patterns represent areas that are comprised fully of land, while in much of original GCM data grid-boxes represents a mix of land and ocean. The total land fraction in the presented spatial patterns is slightly increased, mainly because some mixed land/ocean areas are replaced by land-only estimates to match the UKMO-HadCM3 grid with grid-boxes of either pure land or ocean (see Figure S1). This increases the average grid-box warming, due to diminished
10 representation of the oceanic heat uptake. As a result, the fitting procedure yields regional warming patterns (column "TAS" in Table 3) which, when area-weighted, overall return a value slightly larger than 1.0 K/K. However, this effect has no impact on the global energy budget in the IMOGEN framework, which is resolved independently with EBM.

There are a number of potential methodological enhancements that can be implemented in the next version of
15 the dataset including the way it is utilised by the IMOGEN framework. For example, so far the natural variability around the trend in IMOGEN is simulated through a daily "weather generator" component, under the assumption that the spread remains within the set bounds. However in reality the signal in GCM runs can not only adjust the mean but also the variability itself. This suggests that future research, at least for some variables, additional patterns might be needed that capture variability changes. Furthermore, an extra set of
20 patterns to capture longer-term inter-annual or inter-decadal variability, over and beyond linear changes, could be considered. Model outputs have, until recently, been continuously added to the newer CMIP5 database; pattern-scaling against those newer GCMs can now be undertaken.

Global temperature changes due to atmospheric gas composition that adjusts radiative forcing is achieved through a small number of parameters in a global energy balance model. However aerosols in particular cause
25 problems for this, as the gases are not well-mixed, unlike greenhouse gases. Instead they show strong spatial variation and thus make strong regional variation in radiative forcing, unlike the relatively spatially homogenous greenhouse gases. Shiogama et al. (2010) showed that pattern-scaling is less reliable in the case of precipitation than for temperature in part because precipitation is more sensitive to aerosol forcing. A potential improvement in the presented method in this regard is to use additional spatial masks for aerosol-affected
30 regions.

In terms of many metrics, pattern-scaling is a method that can approximate the vastly more complex GCM frameworks. However this comes with caveats as to its limitations (Good et al., 2015). For example, local climatic feedbacks are not constant in time, and different components of the climate system respond on different timescales (Chadwick & Good, 2013). Nevertheless, as long as used aware of its limitations, its
35 simplicity, availability and computational speed of operation does allow for intermediate analysis before operation of full-complex GCMs with new land surface parameterisation. This paper takes the further step of adding to its capability the scanning across of a large set of GCMs emulated.

In addition to sources of uncertainty which are linked to methods and the assumptions made, there is uncertainty linked directly to input data quality. For example, the decision to use 20C3M and SRES scenario to derive patterns, and the idealised scenario of 1% annual CO_2 increase to calibrate the EBM model, reflects a compromise between the accuracy of patterns and forcings. It could be argued that ideally both the patterns

5 and the calibration parameters should be derived from the same set of GCM runs. However, since the SRES runs are longer (12 decades with part of the 20C3M run), therefore they are a relatively better source for detection of the linear trend (Mitchel 2003), whereas for one-third of GCMs a necessary alternative would be the idealised scenario of 1% annual CO_2 increase to double levels which provides only 7 decades. On the other hand, the idealised CO_2 increase scenarios are a better basis for energy balance model calibration for rigorous

10 studies on the impacts of various CO_2 emission pathways, because the definition of SRES forcings varies between modelling groups (they often encompass atmospheric aerosols) and they are generally poorly documented.

Ultimately, a better dataset is likely to be the CMIP5 ensemble. This formed the basis of the recent 5th IPCC report (IPCC, 2013) using diagnostics available at that time, and is a database only recently completed, has

15 much potential to improve the performance of the described pattern-scaling framework. Aside from the fact that the models themselves have improved, more scenarios are considered, allowing better handling of forcings other than CO_2, and data availability is better. For this reason, the main next enhancement of the IMOGEN system is to migrate over to the CMIP5 dataset. With preparations now starting for the 6th IPCC report, and new simulations being made for that, it is timely to consolidate, and calibrate a new set of patterns for the

20 CMIP5 family of GCMs, building on the analysis presented in this paper.

Data and Code Availability

The IMOGEN version 2.0 patterns and EBM parameters, along with documentation, are available for full download (under "IMOGEN") from the UK Environmental Information Data Centre (EIDC; http://eidc.ceh.ac.uk). The IMOGEN framework (Huntingford et al. 2010) have become a component of the JULES land surface

25 initiative (Best et al., 2011; Clark et al., 2011), and it is available via that route (jules.jchmr.org). For the most up-to-date IMOGEN code, please contact the corresponding author.

Author Contributions

PZ performed the fitting of the patterns and EBM parameters against the CMIP3 database. CH developed the overall IMOGEN model framework. LMM advised on impacts applications and NS aided with context placing of

30 the analysis in terms of other GCM emulation systems. All authors contributed towards writing the manuscript.

References

Atkin, O. K., Bloomfield, K. J., Reich, P. B., Tjoelker, M. G., Asner, G. P., Bonal, D., Bonisch, G., Bradford, M. G., Cernusak, L. A., Cosio, E. G., Creek, D., Crous, K. Y., Domingues, T. F., Dukes, J. S., Egerton, J. J. G., Evans, J. R., Farquhar, G. D., Fyllas, N. M., Gauthier, P. P. G., Gloor, E., Gimeno, T. E., Griffin, K. L., Guerrieri, R., Heskel, M. A., Huntingford, C., Ishida, F. Y., Kattge, J., Lambers, H., Liddell, M. J., Lloyd, J., Lusk, C. H., Martin, R. E., Maksimov, A. P., Maximov, T. C., Malhi, Y., Medlyn, B. E., Meir, P., Mercado, L. M., Mirotchnick, N., Ng, D., Niinemets, U., O'Sullivan, O. S., Phillips, O. L., Poorter, L., Poot, P., Prentice, I. C., Salinas, N., Rowland, L. M., Ryan, M. G., Sitch, S., Slot, M., Smith, N. G., Turnbull, M. H., VanderWel, M. C., Valladares, F., Veneklaas, E. J., Weerasinghe, L. K., Wirth, C., Wright, I. J., Wythers, K. R., Xiang, J., Xiang, S. and Zaragoza-Castells, J.: Global variability in leaf respiration in relation to climate, plant functional types and leaf traits, New Phytol., 206, 614-636, doi:10.1111/nph.13253, 2015.

Best, M. J. Pryor, M., Clark, D. B., Rooney, G. G., Essery, R. L. H., Menard, C. B., Edwards, J., Hendry, M. A., Porson, A., Gedney, N., Mercado, L. M., Sitch, S., Blyth, E., Boucher, O., Cox, P. M., Grimmond, C. S. B. and Harding, R. J.: The Joint UK Land Environment Simulator (JULES), model description - Part 1: Energy and water fluxes, Geosci. Model Dev., 4, 677-699, doi:10.5194/gmd-4-677-2011, 2011.

Cabre, M. F., Solman, S. A. and Nunez, M. N.: Creating regional climate change scenarios over southern South America for the 2020's and 2050's using the pattern scaling technique: validity and limitations, Climatic Change, 98, 449-469, doi:10.1007/s10584-009-9737-5, 2010.

Chadwick, R. and Good, P.: Understanding nonlinear tropical precipitation responses to CO2 forcing, Geophys. Res. Lett., 40, 4911–4915, doi:10.1002/grl.50932, 2013.

Clark, D. B., Mercado, L. M., Sitch, S., Jones, C. D., Gedney, N., Best, M. J., Pryor, M., Rooney, G. G., Essery, R. L. H., Blyth, E., Boucher, O., Harding, R. J., Huntingford, C. and Cox, P. M.: The Joint UK Land Environment Simulator (JULES), model description - Part 2: Carbon fluxes and vegetation dynamics, Geosci. Model Dev., 4, 701-722, doi:10.5194/gmd-4-701-2011, 2011.

24

Cox, P. M., Betts, R. A., Collins, M., Harris, P. P., Huntingford, C. and Jones, C. D.: Amazonian forest dieback under climate-carbon cycle projections for the 21st century, Theor. Appl. Climatol., 78, 137-156, doi:10.1007/s00704-004-0049-4, 2004.

Cox, P. M., Betts, R. A., Jones, C. D., Spall, S. A. and Totterdell, I. J.: Acceleration of global warming due to
5 carbon-cycle feedbacks in a coupled climate model, Nature, 408, 184-187, doi:10.1038/35041539, 2000.

Frieler, K., Meinshausen, M., Mengel, M., Braun, N. and Hare, W.: A scaling approach to probabilistic assessment of regional climate change, J. Clim., 25, 3117-3144, doi:10.1175/JCLI-D-11-00199.1, 2012.

Gedney, N., Cox, P. M. and Huntingford, C.: Climate feedback from wetland methane emissions, Geophys. Res. Lett., 31, L20503, doi:10.1029/2004GL020919, 2004.

10 Good P., Gregory J. M. and Lowe J. A.: A step-response simple climate model to reconstruct and interpret AOGCM projections, Geophys. Res. Lett., 38, L01703, doi:10.1029/2010GL045208, 2011.

Hughes, J. K., Lloyd, A. J., Huntingford, C., Finch, J. W. and Harding, R. J.: The impact of extensive planting of Miscanthus as an energy crop on future CO_2 atmospheric concentrations, Glob. Change Biol. Bioenergy, 2, 79-88, doi:10.1111/j.1757-1707.2010.01042.x, 2010.

15 Huntingford, C., Booth, B. B. B., Sitch, S., Gedney, N., Lowe, J. A., Liddicoat, S. K., Mercado, L. M., Best, M. J., Weedon, G. P., Fisher, R. A., Lomas, M. R., Good, P., Zelazowski, P., Everitt, A. C., Spessa, A. C., Jones, C. D.: IMOGEN: an intermediate complexity model to evaluate terrestrial impacts of a changing climate, Geosci. Model Dev., 3, 679-687, doi:10.5194/gmd-3-679-2010, 2010.

Huntingford, C. and Cox, P. M.: An analogue model to derive additional climate change scenarios from existing
20 GCM simulations, Clim. Dynam., 16, 575-586, doi:10.1007/s003820000067, 2000.

Huntingford, C., Cox, P. M., Mercado, L. M., Sitch, S., Bellouin, N., Boucher, O. and Gedney, N.: Highly contrasting effects of different climate forcing agents on terrestrial ecosystem services, Philos. T. R. Soc. A, 369, 2026-2037, doi:10.1098/rsta.2010.0314, 2011.

Huntingford, C., Harris, P. P., Gedney, N., Cox, P. M., Betts, R. A., Marengo, J. A. and Gash, J. H. C.: Using a GCM
25 analogue model to investigate the potential for Amazonian forest dieback, Theor. Appl. Climatol., 78, 177-185, doi:10.1007/s00704-004-0051-x, 2004.

Huntingford, C., Mercado, L. and Post, E.: Earth Science The timing of climate change, Nature, 502, 174-175, 2013a.

Huntingford, C., Zelazowski, P., Galbraith, D., Mercado, L. M., Sitch, S., Fisher, R., Lomas, M., Walker, A. P.,
30 Jones, C. D., Booth, B. B. B., Malhi, Y., Hemming, D., Kay, G., Good, P., Lewis, S. L., Phillips, O. L., Atkin, O. K., Lloyd, J., Gloor, E., Zaragoza-Castells, J., Meir, P., Betts, R., Harris, P. P., Nobre, C., Marengo, J., Cox, P. M.,

Deleted: Gordon, C., Cooper, C., Senior, C. A., Banks, H., Gregory, J. M., Johns, T. C., Mitchell, J. F. B. and Wood, R. A.: The simulation of SST, sea ice extents and ocean heat transports in a version of the Hadley Centre coupled model without flux adjustments, Clim. Dynam., 16, 147-168, doi:10.1007/s003820050010, 2000.¶

Simulated resilience of tropical rainforests to CO2-induced climate change, Nat. Geosci., 6, 268-273, doi:10.1038/NGEO1741, 2013b.

Huntingford, C., Smith, D. M., Davies, W. J., Falk, R., Sitch, S. and Mercado, L.M..: Combining the ABA and net photosynthesis-based model equations of stomatal conductance, Ecol. Model., 300, 81-88, doi:10.1016/j.ecolmodel.2015.01.005, 2015.

Ines, A. V. M. and Hansen, J. W.: Bias correction of daily GCM rainfall for crop simulation studies, Agr. Forest Meteorol., 138, 44–53, doi:10.1016/j.agrformet.2006.03.009, 2006.

IPCC: Climate Change 2007: The Physical Science Basis. Contribution of Working Group I to the Fourth Assessment Report of the Intergovernmental Panel on Climate Change [Solomon, S., D. Qin, M. Manning, Z. Chen, M. Marquis, K.B. Averyt, M.Tignor and H.L. Miller (eds.)], Cambridge University Press, Cambridge, United Kingdom and New York, NY, USA., 2007.

IPCC: Climate Change 2013: The Physical Science Basis. Contribution of Working Group I to the Fifth Assessment Report of the Intergovernmental Panel on Climate Change [Stocker, T.F., D. Qin, G.-K. Plattner, M. Tignor, S.K. Allen, J. Boschung, A. Nauels, Y. Xia, V. Bex and P.M. Midgley (eds.)], Cambridge University Press, Cambridge, United Kingdom and New York, NY, USA, 1535 pp, doi:10.1017/CBO9781107415324, 2013.

Joos, F., Bruno, M., Fink, R., Siegenthaler, U., Stocker, T.F. and LeQuere, C.: An efficient and accurate representation of complex oceanic and biospheric models of anthropogenic carbon uptake, Tellus B, 48, 397-417, doi:10.1034/j.1600-0889.1996.t01-2-00006.x, 1996.

Kala, J., De Kauwe, M. G., Pitman, A. J., Lorenz, R., Medlyn, B. E., Wang, Y. P., Lin, Y. S. and Abramowitz, G.: Implementation of an optimal stomatal conductance scheme in the Australian Community Climate Earth Systems Simulator (ACCESS1.3b), Geosci. Model Dev., 8, 3877-3889, doi:10.5194/gmd-8-3877-2015, 2015.

Malhi, Y., Aragao, L. E. O. C., Galbraith, D., Huntingford, C., Fisher, R., Zelazowski, P., Sitch, S., McSweeney, C. and Meir, P.: Exploring the likelihood and mechanism of a climate-change induced dieback of the Amazon rainforest, P. Natl. Acad. Sci. USA, 106, 20610–20615, doi:10.1073/pnas.0804619106, 2009.

Medlyn, B. E., Duursma, R. A., Eamus, D., Ellsworth, D. S., Prentice, I. C., Barton, C. V. M., Crous, K. Y., de Angelis, P., Freeman, M. and Wingate, L.: Reconciling the optimal and empirical approaches to modelling stomatal conductance, Glob. Change Biol., 17, 2134-2144, doi:10.1111/j.1365-2486.2010.02375.x, 2011.

Meehl, G. A., Covey, C., Delworth, T., Latif, M., McAvaney, B., Mitchell, J. F. B., Stouffer, R. J. and Taylor, K. E.: The WCRP CMIP3 multimodel dataset – A new era in climate change research, B. Am. Meteorol. Soc., 88, 1383–1394, doi:10.1175/BAMS-88-9-1383, 2007.

Meehl, G. A., T. F. Stocker, W. D. Collins, P. Friedlingstein, A. T. Gaye, J. M. Gregory, A. Kitoh, R. Knutti, J. M. Murphy, A. Noda, S. C. B. Raper, I. G. Watterson, A. J. Weaver and Z.-C. Zhao: Global Climate Projections. In:

Climate Change 2007: The Physical Science Basis. Contribution of Working Group I to the Fourth Assessment Report of the Intergovernmental Panel on Climate Change [Solomon, S., D. Qin, M. Manning, Z. Chen, M. Marquis, K. B. Averyt, M. Tignor and H. L. Miller (eds.)], Cambridge University Press, Cambridge, United Kingdom and New York, NY, USA., 2007.

5   Mercado, L. M., Bellouin, N., Sitch, S., Boucher, O., Huntingford, C., Wild, M. and Cox, P. M.: Impact of changes in diffuse radiation on the global land carbon sink, Nature, 458, 1014-U87, doi:10.1038/nature07949, 2009.

Mercado, L. M., Huntingford, C., Gash, J. H. C., Cox, P. M. and Jogireddy, V.: Improving the representation of radiation interception and photosynthesis for climate model applications, Tellus B, 59, 553-565, doi:10.1111/j.1600-0889.2007.00256.x, 2007.

10   Mercado, L. M., Patino, S., Domingues, T. F., Fyllas, N. M., Weedon, G. P., Sitch, S., Quesada, C. A., Phillips, O. L., Aragao, L. E. O. C., Malhi, Y., Dolman, A. J., Restrepo-Coupe, N., Saleska, S. R., Baker, T. R., Almeida, S., Higuchi, N. and Lloyd, J.: Variations in Amazon forest productivity correlated with foliar nutrients and modelled rates of photosynthetic carbon supply, Philos. T. R. Soc. B, 366, 3316-3329, doi:10.1098/rstb.2011.0045, 2011.

Mercado L. M, et al., Sensitivity of future land carbon storage to thermal

15   acclimation of photosynthesis in climate-carbon cycle models. In Preparation.

Mitchell, J. F. B., Johns, T. C., Eagles, M., Ingram, W. J. and Davis, R. A.: Towards the construction of climate change scenarios, Climatic Change, 41, 547-581, doi:10.1023/A:1005466909820, 1999.

Mitchell, T. D.: Pattern scaling - An examination of the accuracy of the technique for describing future climates, Climatic Change, 60, 217-242, doi:10.1023/A:1026035305597, 2003.

20   Mitchell, T. D. and Jones, P. D.: An improved method of constructing a database of monthly climate observations and associated high-resolution grids, Int. J. Climatol., 25, 693-712, doi:10.1002/joc.1181, 2005.

Moorcroft, P. R., Hurtt, G. C. and Pacala, S. W.: A method for scaling vegetation dynamics: The ecosystem demography model (ED), Ecol. Monogr., 71, 557-585, doi:10.1890/0012-9615(2001)071[0557:AMFSVD]2.0.CO;2, 2001.

25   Nakićenović, N., Alcamo, J., Davis, G. et al: IPCC Special Report on Emissions Scenarios,

Cambridge University Press, Cambridge, UK, 570 pp., 2000.

Shiogama, H., Emori, S., Takahashi, K., Nagashima, T., Ogura, T., Nozawa, T. and Takemura, T.: Emission scenario dependency of precipitation on global warming in the MIROC3.2 model, J. Climate, 23, 2404-2417, doi:10.1175/2009JCLI3428.1, 2010.

Deleted: ., Shiogama, H

Sitch, S., Cox, P. M., Collins, W. J. and Huntingford, C.: Indirect radiative forcing of climate change through ozone effects on the land-carbon sink, Nature, 448, 791-U4, doi:10.1038/nature06059, 2007.

Sitch, S., Huntingford, C., Gedney, N., Levy, P. E., Lomas, M., Piao, S. L., Betts, R., Ciais, P., Cox, P., Friedlingstein, P., Jones, C. D., Prentice, I. C. and Woodward, F. I.: Evaluation of the terrestrial carbon cycle,
5   future plant geography and climate-carbon cycle feedbacks using five Dynamic Global Vegetation Models (DGVMs), Glob. Change Biol., 14, 2015-2039, doi: 10.1111/j.1365-2486.2008.01626.x, 2008.

Smith, B., Prentice, I. C., and Sykes, M. T.: Representation of Vegetation Dynamics in the Modelling of Terrestrial Ecosystems: Comparing Two Contrasting Approaches within European Climate Space, Global Ecol. and Biogeogr., 10, 621-637, doi:10.1046/j.1466-822X.2001.t01-1-00256.x, 2001.

10   Smith, N. G. and Dukes, J. S.: Plant respiration and photosynthesis in global-scale models: incorporating acclimation to temperature and CO2, Glob. Change Biol., 19, 45–63, doi:10.1111/j.1365-2486.2012.02797.x, 2013.

Sperry, J. S., Wang, Y., Wolfe, B. T., Mackay, D. S., Anderegg, W. R. L., McDowell, N. G. and Pockman, W. T.: Pragmatic hydraulic theory predicts stomatal responses to climatic water deficits, New Phytol., doi:
15   10.1111/nph.14059, 2016.

Taylor, K. E., Stouffer, R. J. and Meehl, G. A.: An overview of CMIP5 and the experiment design, B. Am. Meteorol. Soc., 93, 485-498, doi:10.1175/BAMS-D-11-00094.1, 2012.

Verheijen L. M., Aerts, R., Brovkin, V., Cavender-Bares, J., Cornelissen, J. H. C., Kattge, J. and Van Bodegom, PM: Inclusion of ecologically based variation in plant functional types reduces the projected land carbon sink in an
20   earth system model, Glob. Change Biol., 21, 3074-3086, doi: 10.1111/gcb.12871, 2015.

Wigley, T. M. L., Raper, S. C. B., Smith, S. and Hulme, M.: The Magicc/ScenGen Climate Scenario Generator: version 2.4, Technical manual. CRU, UEA, Norwich, U.K., 2000.

Zaehle, S., Friedlingstein, P. and Friend, A. D.: Terrestrial nitrogen feedbacks may accelerate future climate change, Geophys. Res. Lett., 37, L01401, doi:10.1029/2009GL041345, 2010.

25   Zelazowski, P., Malhi, Y., Huntingford, C., Sitch, S. and Fisher, J. B.: Changes in the potential distribution of humid tropical forests on a warmer planet, Philos. T. R. Soc. A, 369, 137-160, doi:10.1098/rsta.2010.0238, 2011.

28

Table 1. Availability of WCRP CMIP3 data for the climate patterns study, and characteristics of models' depiction of land and water areas (variable sftlf). Land/water transition is either continuous (*cont.*) or abrupt (binary mask - *bin.*). The first characteristic in column "Land mask" pertains to coastlines, whereas the second – to inland waters. The codes in column "Data gaps and issues" are: M – missing, E – 4D variable (surface values need to be extrapolated), G – data gaps, R – some data needed resizing.

	GCM name	Origin	Land mask	Resolution	Data gaps and issues
1.	BCCR-BCM2.0	Norway	cont./cont.	64x128	E (HUR)
2.	CGCM3.1(T47)	Canada	bin./bin.	48x96	E (HUR)
3.	CNRM-CM3	France	bin./bin.	64x128	E (HUR)
4.	CSIRO-Mk3.0	Australia	bin./bin.	96x192	M (UAS, VAS, PS)
5.	CSIRO-Mk3.5	Australia	bin./bin.	96x192	E (HUR)
6.	GFDL-CM2.0	USA	cont./bin.	90x144	E (HUR)
7.	GFDL-CM2.1	USA	cont./bin.	90x144	E (HUR)
8.	GISS-EH	USA	bin./cont.	46x72	E (HUR)
9.	GISS-ER	USA	bin./cont.	46x72	E (HUR), M (RLDS)
10.	FGOALS-g1.0	China	cont./bin.	60x128	E (HUR)
11.	INGV-SXG	Italy	bin./bin.	160x320	E (HUR, UAS, VAS), M (RLDS, RSDS)
12.	INM-CM3.0	Russia	bin./bin.	45x72	E (HUR)
13.	IPSL-CM4	France	cont./bin.	72x96	E (HUR)
14.	MIROC3.2(hires)	Japan	cont./cont.	160x320	E (HUR)
15.	MIROC3.2(medres)	Japan	cont./bin.	64x128	E (HUR)
16.	ECHO-G	Germany-Korea	bin/bin.	48x96	M (HUR)
17.	ECHAM5/MPI-OM	Germany	cont./bin.	96x192	E (HUR)
18.	MRI-CGCM2.3.2	Japan	cont./cont.	64x128	E (HUR) G (PRSN)
19.	CCSM3	USA	cont./bin.	128x256	E (HUR, UAS, VAS)
20.	PCM	USA	cont./bin.	64x128	E (HUR, UAS, VAS)

21.	UKMO-HadCM3	UK	bin/bin.	73x96	E (HUR)
22.	UKMO-HadGEM1	UK	cont./bin.	145x192	E (HUR), R (UAS,VAS)

Table 2. Calibration parameters of the simple IMOGEN Energy Balance Model, for each considered Global Circulation Model. The first column presents which runs (experiments) were used to derive the parameters, listed in the following columns: (i) an ocean effective thermal diffusivity which determines the uptake of energy, κ (Wm^{-1}K^{-1}), (ii) a constant ratio of mean land and ocean surface (SST) rate of warming, ν, (iii-iv) climate sensitivity over land λ_l and ocean λ_o (W m^{-2} K^{-1}), and (v) f, which is a land fraction, including Antarctica, f. The last column presents GCM-specific ratios of warming aver all land per degree of global warming.

	GCM	Calibration basis	Pattern basis	λl	λo	κ	ν	f	$\Delta T_l/°K$
1.	BCCR-BCM2.0	pictrl, 1% to2x	SRES A2	2.00	2.30	350	1.40	0.28	1.26
2.	CGCM3.1(T47)	pictrl, 1% to4x	SRES A2	1.50	1.30	270	1.50	0.31	1.30
3.	CNRM-CM3	pictrl, 1% to4x	SRES A2	1.65	1.58	500	1.46	0.28	1.29
4.	CSIRO-Mk3.0	pictrl, 1% to2x	SRES A2	1.20	1.25	2800	1.69	0.29	1.41
5.	CSIRO-Mk3.5	pictrl, 1% to2x	SRES A2	1.35	0.80	1300	1.58	0.29	1.35
6.	GFDL-CM2.0	pictrl, 1% to4x	SRES A2	1.15	1.70	510	1.53	0.30	1.32
7.	GFDL-CM2.1	pictrl, 1% to4x	SRES A2	1.15	2.05	460	1.58	0.30	1.35
8.	GISS-EH	pictrl, 1% to2x	SRES A1B	1.30	1.65	520	1.48	0.29	1.30
9.	GISS-ER	pictrl, 1% to4x	SRES A2	1.05	1.40	1200	1.61	0.29	1.37
10.	FGOALS-g1.0	pictrl, 1% to2x	SRES A1B	1.80	2.80	11000	1.47	0.30	1.46
11.	INGV-SXG	pictrl, 1% to4x	SRES A2	0.70	1.90	320	1.65	0.28	1.39
12.	INM-CM3.0	pictrl, 1% to4x	SRES A2	1.35	1.70	500	1.50	0.30	1.30
13.	IPSL-CM4	pictrl, 1% to4x	SRES A2	1.00	1.10	700	1.57	0.30	1.34
14.	MIROC3.2(hires)	pictrl, 1% to2x	SRES A1B	1.00	0.70	510	1.38	0.29	1.24
15.	MIROC3.2(medres)	pictrl, 1% to4x	SRES A2	0.83	1.00	720	1.57	0.29	1.35
16.	ECHO-G	pdctrl, 1% to4x	SRES A2	1.05	1.80	50	1.76	0.29	1.45
17.	ECHAM5/MPI-OM	pictrl, 1% to4x	SRES A2	0.86	0.95	500	1.60	0.29	1.36
18.	MRI-CGCM2.3.2	pdctrl, 1% to4x	SRES A2	1.68	1.25	380	1.38	0.30	1.22
19.	CCSM3	pdctrl, 1% to4x	SRES A2	1.10	1.70	1200	1.47	0.29	1.29
20.	PCM	pdctrl, 1% to4x	SRES A2	1.95	2.30	720	1.43	0.29	1.27
21.	UKMO-HadCM3	pictrl, 1% to2x	SRES A2	0.40	1.85	270	1.78	0.29	1.45
22.	UKMO-HadGEM1	pictrl, 1% to4x	SRES A2	0.92	1.46	480	1.60	0.29	1.36
	All			1.23±0.40	1.57±0.51	1148±2220	1.55±0.11	0.29±0.01	1.34±0.06

31

Table 3. Mean climate change patterns (change in quantity per degree of global warming). Values in italics are across-ensemble averages used to fill in data gaps. In these cases, the Percentage Variance Explained statistic was not calculated. Across-variables summary values (last column) which concern incomplete sets of variables are in square brackets.

	GCM name	TAS	HUR	UAS+VAS	RLDS	RSDS	PR	PRSN	PS	ALL
1.	BCCR-BCM2.0	1.0463 (83.04)	-0.0201 (13.29)	0.0089 (2.66)	5.6754 (76.51)	-0.6185 (9.73)	0.0300 (8.16)	-0.0025 (13.14)	0.2324 (30.70)	29.65
2.	CGCM3.1(T47)	1.0561 (85.79)	0.0974 (19.80)	0.0197 (8.30)	6.0605 (87.28)	-0.4722 (18.82)	0.0448 (18.71)	-0.0015 (16.66)	0.0730 (21.33)	34.59
3.	CNRM-CM3	1.0371 (86.64)	-0.0111 (24.84)	0.0098 (8.73)	5.7499 (81.41)	-0.4978 (19.65)	0.0255 (17.05)	0.0000 (17.35)	0.1838 (38.48)	36.77
4.	CSIRO-Mk3.0	1.0740 (82.73)	-0.2354 (13.99)	*0.0108 (-)*	5.9023 (84.39)	-0.6072 (24.46)	0.0165 (9.38)	-0.0032 (25.70)	*0.0947 (-)*	[40.11]
5.	CSIRO-Mk3.5	1.0270 (87.73)	-0.2214 (17.04)	0.0059 (6.93)	6.2917 (87.92)	-0.3596 (25.23)	0.0044 (12.42)	-0.0035 (17.22)	0.0138 (21.94)	34.56
6.	GFDL-CM2.0	1.0731 (83.58)	-0.2653 (14.77)	0.0071 (8.25)	6.0471 (83.69)	-1.8451 (34.58)	0.0042 (16.89)	-0.0041 (21.49)	0.0657 (24.35)	35.95
7.	GFDL-CM2.1	1.0794 (79.71)	-0.2310 (17.35)	0.0113 (9.59)	6.2023 (82.62)	-1.7225 (33.21)	-0.0017 (17.93)	-0.0067 (18.66)	0.2057 (29.21)	36.03
8.	GISS-EH	1.0543 (75.71)	0.0080 (10.48)	0.0103 (4.25)	6.6734 (77.09)	-1.4802 (1.95)	0.0415 (11.28)	-0.0016 (8.04)	0.0264 (12.18)	25.12
9.	GISS-ER	1.0365 (80.07)	-0.1572 (17.25)	0.0099 (7.08)	*6.1883 (-)*	-0.9399 (11.05)	0.0384 (14.76)	-0.0018 (10.16)	0.0251 (18.31)	[22.67]
10.	FGOALS-g1.0	1.1180 (83.05)	-0.0980 (4.11)	-0.0031 (1.36)	6.3137 (82.71)	-0.9748 (9.67)	0.0205 (6.70)	-0.0010 (15.52)	0.0836 (13.62)	27.09
11.	INGV-SXG	1.0863 (88.01)	-0.0209 (22.96)	0.0128 (5.20)	*6.2418 (-)*	*-0.7667 (-)*	0.0184 (10.68)	-0.0067 (19.10)	0.0217 (18.58)	35.98
12.	INM-CM3.0	1.0604 (83.51)	-0.0391 (15.44)	0.0130 (4.88)	5.7124 (78.17)	-0.2908 (23.54)	0.0200 (14.32)	-0.0071 (12.97)	0.0124 (16.43)	31.16
13.	IPSL-CM4	1.1043 (90.18)	-0.6717 (27.46)	0.0059 (9.92)	6.1517 (85.26)	0.0932 (27.85)	0.0166 (15.72)	-0.0089 (23.73)	0.1216 (21.31)	37.68
14.	MIROC3.2(hires)	1.0801 (94.19)	-0.1528 (16.89)	0.0031 (8.45)	6.2088 (92.28)	-1.0731 (36.21)	0.0271 (20.90)	-0.0052 (25.45)	0.2352 (37.87)	41.53
15.	MIROC3.2(medres)	1.1281 (91.16)	-0.2819 (15.56)	0.0062 (9.38)	6.4687 (88.97)	-1.7130 (38.30)	0.0272 (22.37)	-0.0032 (23.53)	0.1417 (30.26)	39.94
16.	ECHO-G	1.1383 (88.41)	*-0.1256 (-)*	0.0165 (9.54)	6.5682 (86.84)	-1.4149 (20.41)	0.0574 (18.77)	-0.0046 (21.54)	-0.0648 (19.65)	[37.88]
17.	ECHAM5/MPI-OM	1.0726 (89.81)	-0.2200 (18.66)	0.0173 (8.35)	6.1048 (89.35)	-0.3009 (18.78)	0.0294 (14.08)	-0.0052 (17.45)	0.0714 (22.61)	34.89
18.	MRI-CGCM2.3.2	1.0641 (84.62)	0.6378 (13.21)	-0.0048 (3.25)	6.5956 (82.92)	-1.2903 (10.43)	0.0387 (7.60)	*-0.0063 (-)*	0.0979 (17.37)	[31.34]
19.	CCSM3	1.1182 (87.92)	-0.0307 (15.09)	0.0091 (6.75)	6.8102 (89.67)	-1.2080 (24.48)	0.0477 (21.47)	-0.0071 (20.45)	0.1629 (25.02)	36.36
20.	PCM	1.1059 (78.64)	0.0704 (9.65)	0.0346 (1.13)	6.2678 (75.20)	-0.9678 (8.34)	0.0573 (12.52)	0.0009 (13.56)	0.1509 (17.32)	27.04

Deleted: assembly

#										
21.	UKMO-HadCM3	1.0572 (86.57)	-0.7051 (29.40)	0.0137 (9.85)	5.6891 (84.81)	0.2089 (27.15)	0.0096 (16.36)	-0.0036 (15.88)	-0.0542 (23.05)	36.63
22.	UKMO-HadGEM1	1.1222 (88.60)	-0.0900 (18.05)	0.0190 (15.49)	6.2180 (89.33)	-1.9194 (37.04)	0.0076 (21.45)	-0.0039 (22.27)	0.1814 (32.21)	40.55
	ALL	1.079 ±0.032 (85.44 ±4.37)	-0.1256 ±0.2579 (16.92 ±5.71)	0.0108 ±0.0080 (7.11 ±3.32)	6.188 ±0.400 (84.74 ±4.97)	-0.9164 ±0.6000 (23.29 ±10.23)	0.0264 ±0.0165 (14.98 ±4.61)	-0.0040 ±0.0025 (17.96 ±4.67)	0.095 ±0.084 (23.33 ±6.99)	(34.25 ±5.21)
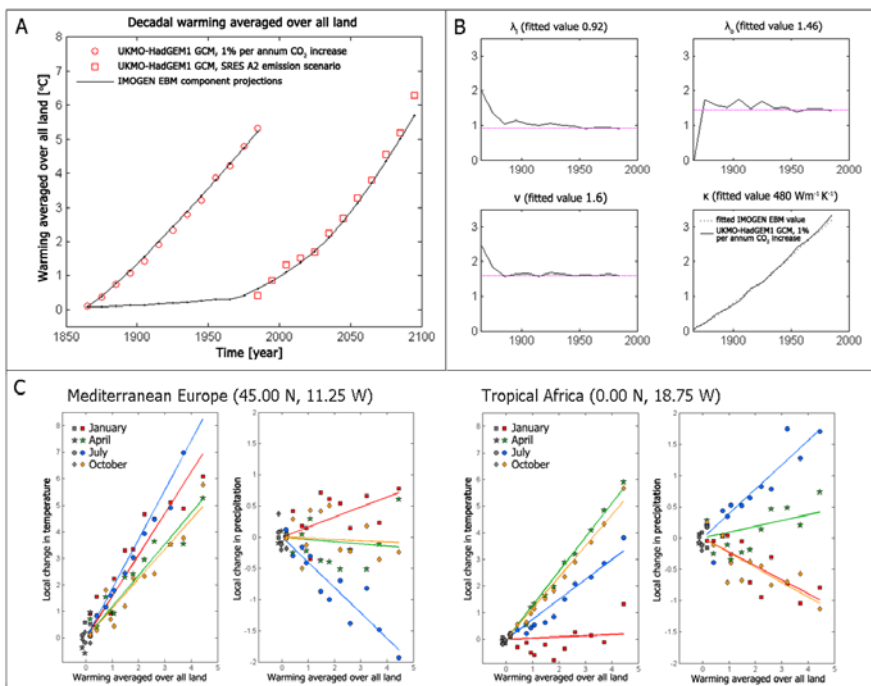
Figure 1: Illustration of the process leading to parameterization of the IMOGEN Energy Balance Model and the scaled climate patterns (together forming the "pattern scaling set"), based on the example of the UKMO-HadGEM1 GCM. A: emulation of a warming pathway across time. The 1% to quadrupling atmospheric CO_2 run was used for calibration of the energy balance model while the SRES A2 scenario run was used to validate the results. B: Fitting of the individual EBM parameters, underlining the match presented in A. Climate sensitivities over land λ_l and ocean λ_o, as well as the ratio of land to ocean warming rate, v, (pink lines) are derived directly from GCM run data (black curves, 1% run). The fourth parameter, an ocean effective thermal diffusivity, κ, determines modelled oceanic temperature profile. The κ value is selected based upon comparing calculated values of top-of-profile temperature against global mean SST changes projected by UKMO-HadGEM1 1% run (shown). C: Example local fitting of patterns of temperature and precipitation, found as regression coefficients (coloured straight lines) against calculated changes in mean temperature over land from UKMO-HadGEM1. Two representative grid-boxes in Mediterranean Europe and Tropical Africa are shown. Coloured symbols are decadal mean monthly values from the UKMO-HadGEM1 SRES A2 run, whilst the grey markers represent data from the 20C3M simulation, which were used to normalize to temperature and precipitation change, and are also corresponding to CRU normals (years 1961–90). Regression "pattern" fit is forced through [0,0] point, as in diagrams.
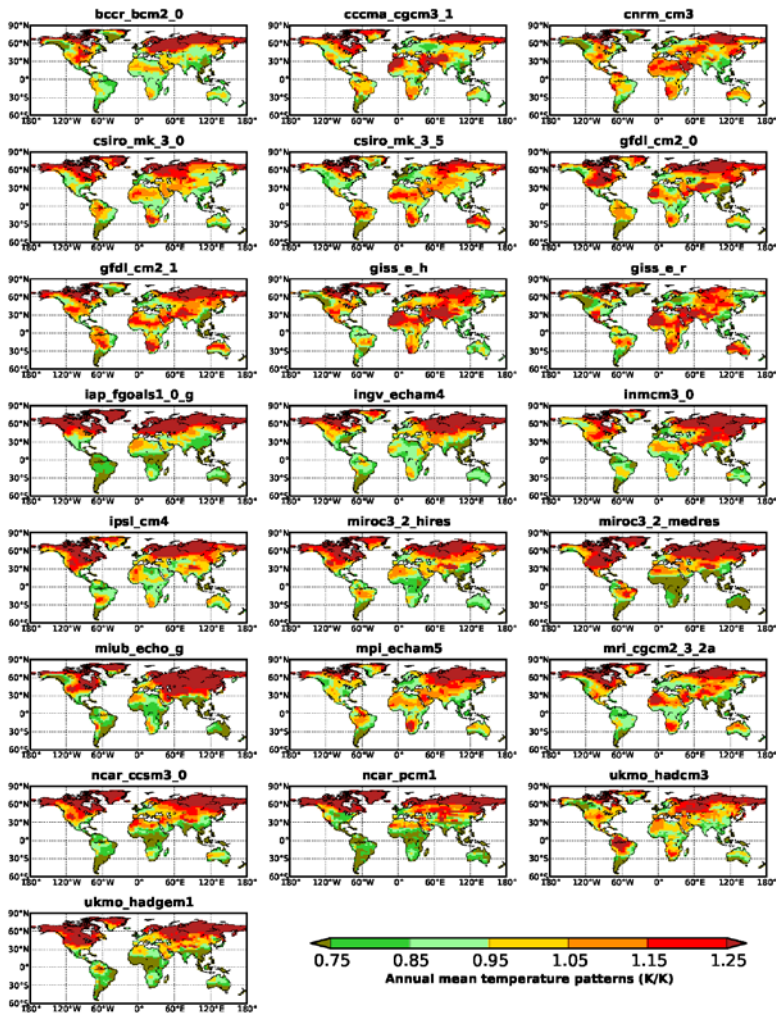
34

Figure 2: Annual means of the monthly patterns of local temperature change per degree warming over all land (K K^{-1}). Data presented for 22 GCMs considered in this study.
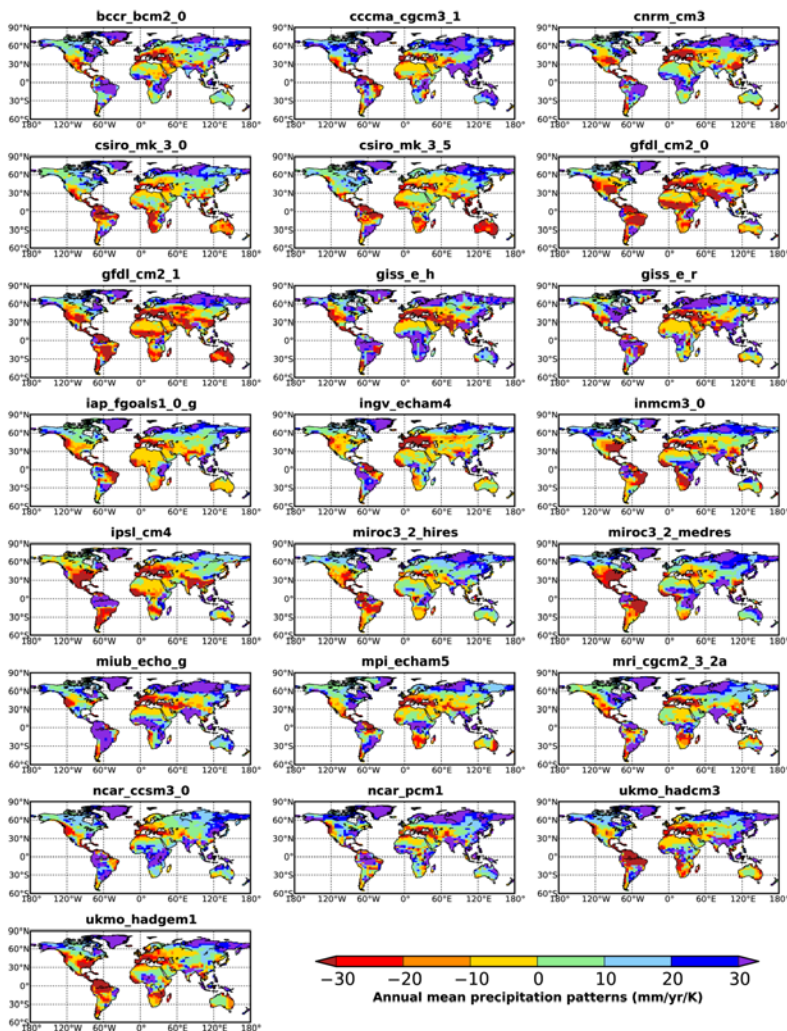
Figure 3: Annual means of the monthly patterns of local precipitation change per degree warming over all land (mm yr^{-1} K^{-1}). Data presented for 22 GCMs considered in this study.
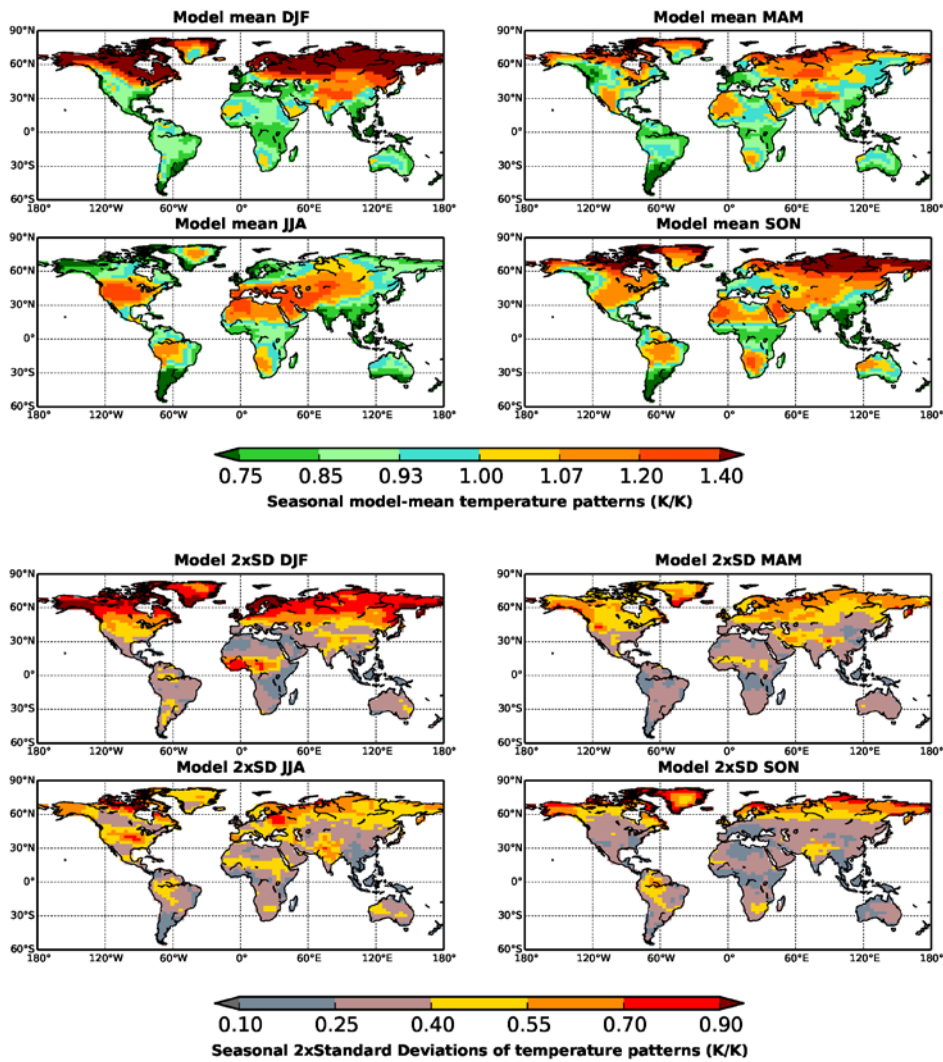
*Figure 4: Seasonal means and variation (2*SD) of the monthly patterns of local temperature change per degree warming over all land (K K⁻¹), across 22 GCMs.*
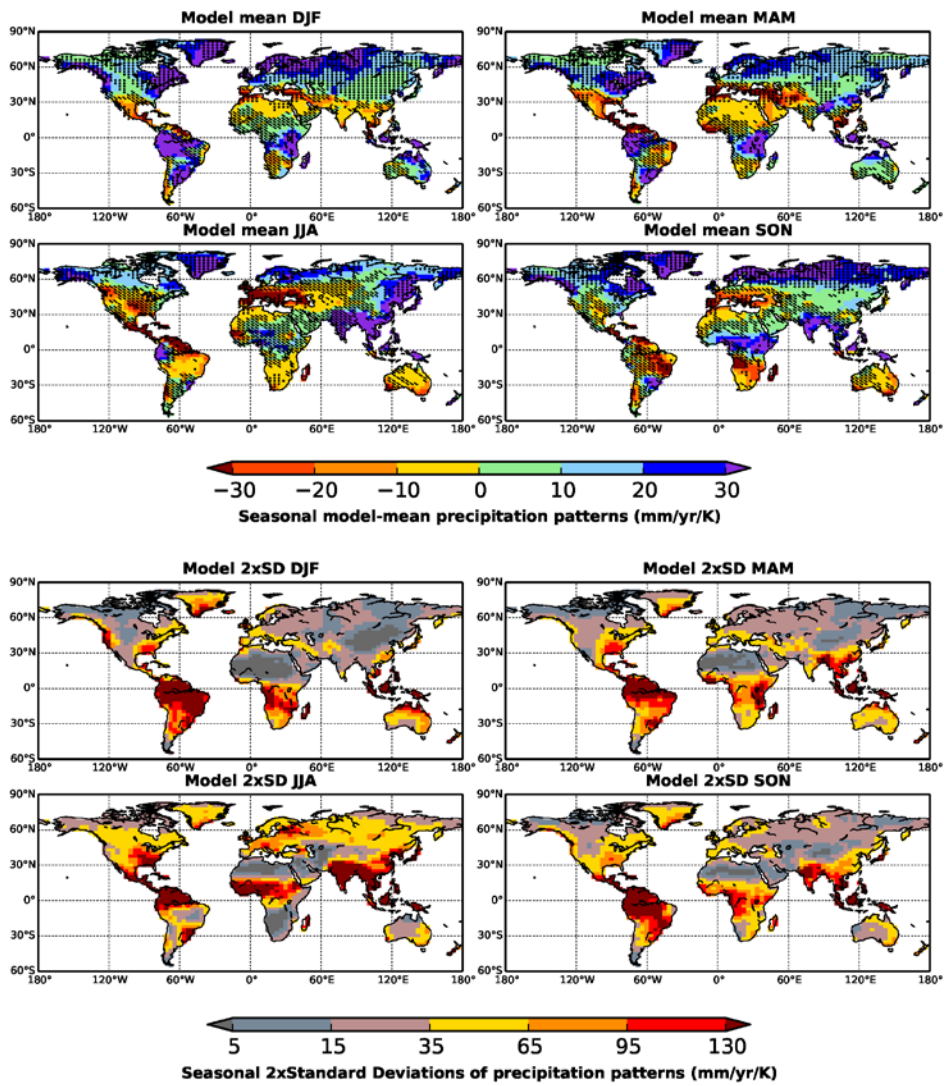
*Figure 5: Seasonal means and variation (2*SD) in the monthly patterns of local precipitation change per degree warming over all land (mm yr-1 K-1), across 22 GCMs. In regions marked with stippling more than 66% of the models agree in the sign of the change.*
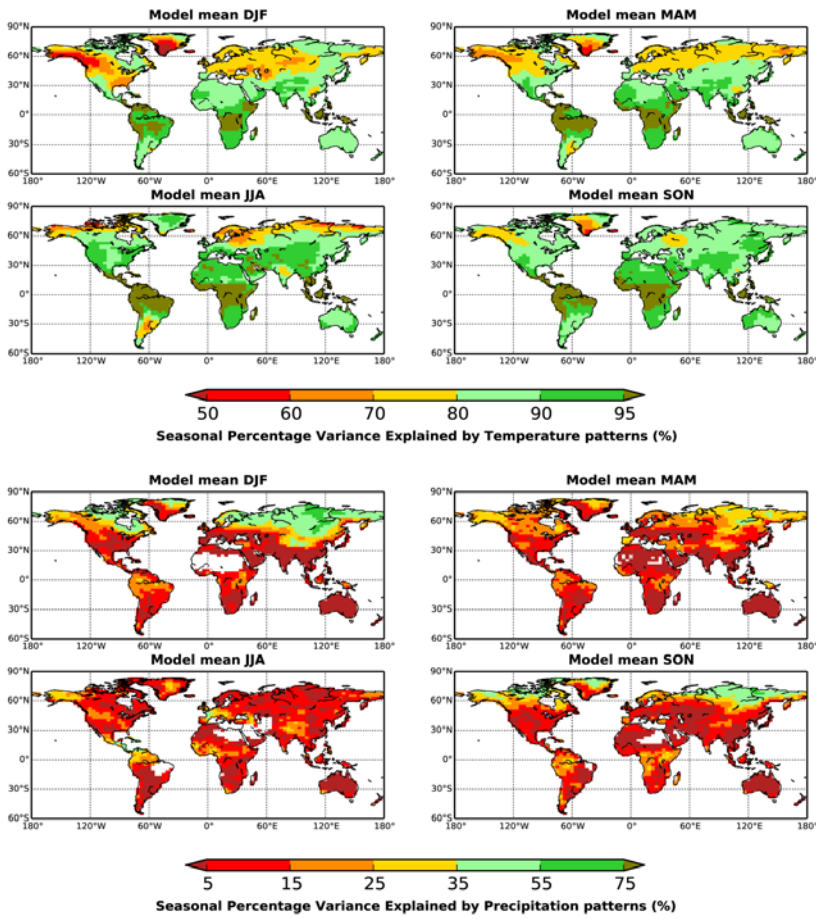
Figure 6: Seasonal coefficient of determination (COD) of the monthly patterns of local temperature and precipitation change per degree warming, across 22 GCMs.
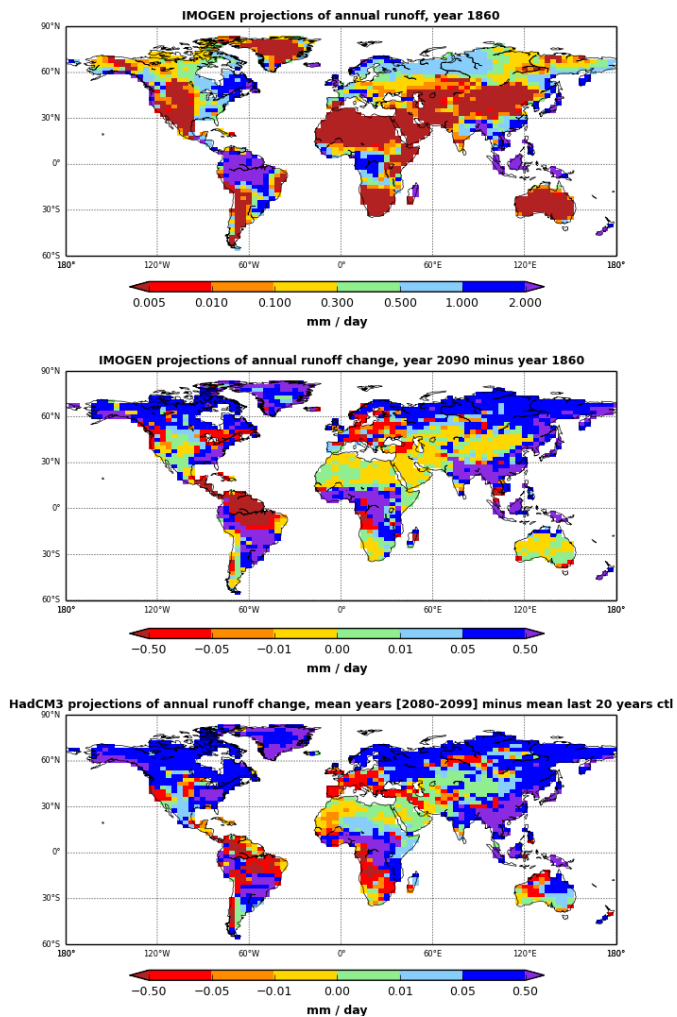
Figure 7: Estimates of gridbox mean annual total runoff, R_{tot} (mm/day). Top panel: for IMOGEN and year 1860; middle panel: IMOGEN estimates and year 2090 calculations of R_{tot} minus those of year 1860; bottom panel: HadCM3 estimates and mean of year 2080-2099 calculations of R_{tot} minus those of mean of last 20 years of pre-industrial control simulation.
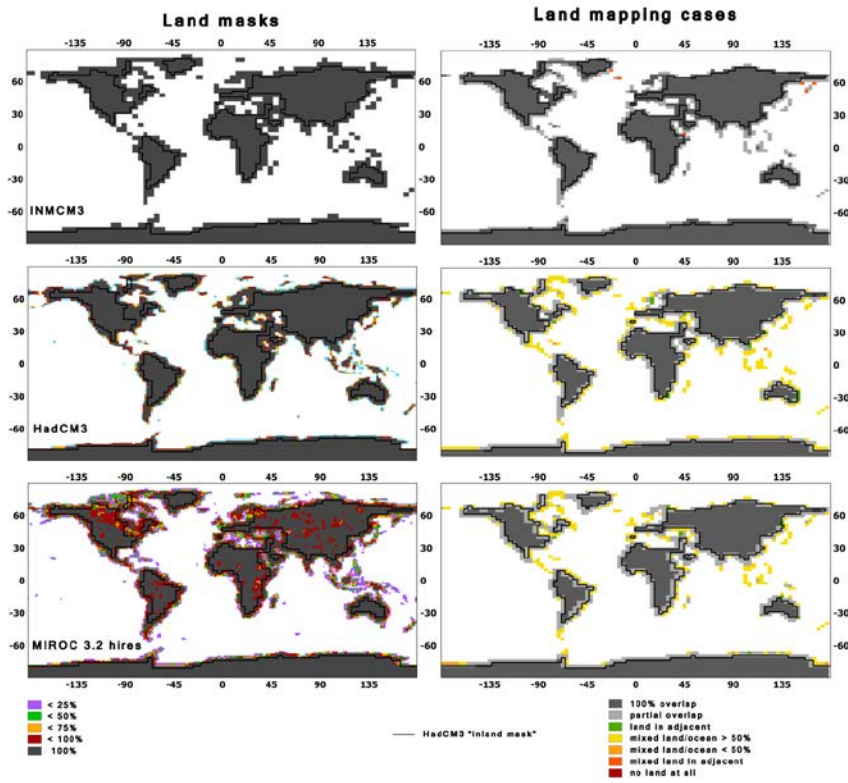
Supplementary Information

Figure S1. Three examples of GCM grids (on the left), representing main grid categories in the CMIP3 dataset. Diagrams on the right show where different re-gridding strategies were applied in order to translate each grid-box into the UKMO-HadCM3 GCM land grid-boxes.
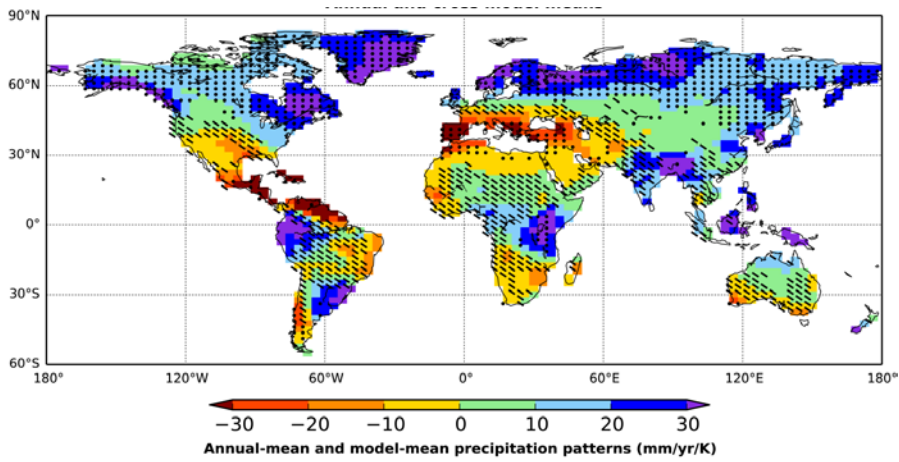
Figure S2. Annual means and variation (2*SD) in the monthly patterns of local precipitation change per degree warming over all land (mm yr-1 K-1), across 22 GCMs. In regions marked with stippling more than 66% of the models agree in the sign of the change. This figure has been prepared to enable comparison with Figure 10.9 in Meehl et al (2007).

Table S1. Type of overlap between land grid-boxes of the UKMO-HadCM3 grid and corresponding areas across other 22 GCM considered in this study.

	Mapping case	Number of cases	Fraction of the dataset
1	only 100% land overlaid and averaged	32900	0.6281
2	some 100% land overlaid and averaged (ocean and mixed areas)	14012	0.2675
3	100% land found in the neighbourhood and 100% land cases averaged	119	0.0023
4	no 100% land in the neighbourhood found, so take mixed land (frac>=0.5) from the grid-box	5109	0.0975
5	no 100% land in the neighbourhood found, so take mixed land (frac>0) from the grid-box	183	0.0035
6	no 100% land in the neighbourhood found, nor mixed land in the grid-box, but mixed land in the neighbourhood	6	0.0001
7	no land at all found (so simple averaging done)	53	0.0010

Supplementary Material

S1. Files containing climate change patterns

The final climate pattern scaling set is available in two versions: A: with precipitation normalised (file pattRelPrFin_v3c.zip, see Data and Methods), and B: without normalisation (file pattFin_v3c.zip).

Each of the two dataset versions contains 22 directories with named after GCMs considered in this study (pattRelPR_d2_GCMNAME and patt_d2_GCMNAME in version A and B, respectively). Each directory contains 12 ASCII text files with names corresponding to months they represent. Each file contains a one-line header followed by 1631 lines, each one containing patterns for a single location. Meaning of consecutive columns is as follows:

1. Longitude, 2. Latitude, 3. TAS pattern, 4. HUR at surface pattern, 5. Wind (UAS+VAS) pattern, 6. (empty), 7. RLDS pattern, 8. RSDS pattern, 9. (empty), 10. PR pattern, 11. PRSN, 12. PS pattern, 13. (empty)

IMOGEN EBM calibration parameters are given in Table 2.

The files can be downloaded from the UK Environmental Information Data Centre (EIDC; http://eidc.ceh.ac.uk)

Deleted: at:	

S2. Homogenisation of GCM resolutions and land masks

GCMs differ between each other in terms of how precisely they represent the Earth surface's detail (as represented in the "land mask" variable SFTLF). Spatial resolution of these data varies between GCMs (Table 1), ranging from hundreds of kilometres (e.g. GISS models, or INM-CM3.0) to around 50 km (e.g. MIROC3.2hires). Concerning grid spacing, data are mapped on either a regular or a Gaussian grid. In addition, GCM grid-boxes are split into land and water in a number of ways (see below). This diversity of output spatial properties alone imposes a challenge for data end-users, including policymakers.

Deleted: ESM
Deleted: ESM
Deleted: ESM

Implementation of CMIP3 patterns in the IMOGEN system included transforming all types of WCRP CMIP3 grids into one, which was chosen to be the UKMO-HadCM3, based on the need for compatibility with previous applications of the tool.

There are four types of land mask: (i) binary (each grid box is100% land, or 100% water, e.g. UKMO-HadCM3), (ii) continuous without inland waters (from 0% to 100% of land, e.g. UKMO-HadGEM1), (iii) binary for oceans, continuous for inland waters (e.g. GISS models), (iv) continuous with inland waters (MIROC3.2(hires)). This is important because the IMOGEN tool was originally designed to model impact over land (excluding Antarctica), assuming different warming rate for land and ocean areas, and therefore the climate patterns used to drive it need to apply to land as much as possible. In order to achieve that, the following procedure was implemented.

First, spatial resolution of CMIP3 data was homogenized to 1 x 1 degree through bilinear interpolation. Subsequently, the data were re-mapped onto the HadCM3 model grid with binary representation of land and ocean and no inland freshwater bodies. The mapping procedure distinguishes between land, ocean and mixed areas, and allows for minor spatial shifts in grid boxes in order to preserve the land/ocean contrast in surface variables. Since the initial 1 x 1degree resolution is finer than in the HadCM3 grid, this enables the procedure of segregation of fine grid-boxes overlapping with a particular HadCM3 land grid-box, according to the proportion of land they represent. When '100%' land fine grid-boxes are present, only these are averaged and assigned the HadCM3 grid-box. Fractional land grid-boxes are used in the absence of 100% land and in the rare

cases when no land overlaps with the HadCM3 land grid-box then the immediate neighbourhood is included in the procedure. Land areas represented in the final output may exhibit a significantly altered behaviour (in terms of mean surface temperature and Top-Of-Atmosphere radiative fluxes); however, this dataset is only used to characterise 'pure' land occurring within, or nearby, each grid-box, while the assessment of global changes in temperature, or modelling of the energy balance of land and ocean is done using AOGCM data in its original format.

Relationship between the radiative forcing due to CO_2 increase and the surface temperature increase over land and ocean is derived based on the original GCM data, before its mapping onto UKMO-HadCM3 grid. It relies on the decoupling of energy fluxes over land and oceans, which in the 'continuous' grids is hampered into a small extent because of the existence of grid-boxes containing both land and ocean, where partitioning of energy fluxes between land and ocean with full certainty is not possible. In the case of a few grids which represent inland fresh water, the UKMO-HadCM3 representation of inland was used to over-write the original land fraction values.

S3. Trends in annual precipitation change - comparison with IPCC data

References (Supplementary Material)

Cox, P. M., Betts, R. A., Collins, M., Harris, P. P., Huntingford, C. and Jones, C.D.: Amazonian forest dieback under climate-carbon cycle projections for the 21st century, Theor. Appl. Climatol., 78, 137-156, doi:10.1007/s00704-004-0049-4, 2004.

Cox, P. M., Betts, R. A., Jones, C. D., Spall, S. A. and Totterdell, I. J.: Acceleration of global warming due to carbon-cycle feedbacks in a coupled climate model, Nature, 408, 184-187, doi:10.1038/35041539, 2000.

Hughes, J. K., Lloyd, A. J., Huntingford, C., Finch, J. W. and Harding, R. J.: The impact of extensive planting of Miscanthus as an energy crop on future CO2 atmospheric concentrations, Glob. Change Biol. Bioenergy, 2, 79-88, doi:10.1111/j.1757-1707.2010.01042.x, 2010.

Huntingford, C., Booth, B. B. B., Sitch, S., Gedney, N., Lowe, J. A., Liddicoat, S. K., Mercado, L. M., Best, M. J., Weedon, G. P., Fisher, R. A., Lomas, M. R., Good, P., Zelazowski, P., Everitt, A. C., Spessa, A. C., Jones, C. D.: IMOGEN: an intermediate complexity model to evaluate terrestrial impacts of a changing climate, Geosci. Model Dev., 3, 679-687, doi:10.5194/gmd-3-679-2010, 2010.

Huntingford, C. and Cox, P. M.: An analogue model to derive additional climate change scenarios from existing GCM simulations, Clim. Dynam., 16, 575-586, doi:10.1007/s003820000067, 2000.

Huntingford, C., Cox, P. M., Mercado, L. M., Sitch, S., Bellouin, N., Boucher, O. and Gedney, N.: Highly contrasting effects of different climate forcing agents on terrestrial ecosystem services, Philos. T. R. Soc. A, 369, 2026-2037, doi:10.1098/rsta.2010.0314, 2011.

Huntingford, C., Smith, D. M., Davies, W. J., Falk, R., Sitch, S. and Mercado, L.M..: Combining the ABA and net photosynthesis-based model equations of stomatal conductance, Ecol. Model., 300, 81-88, doi:10.1016/j.ecolmodel.2015.01.005, 2015.

IPCC: The Physical Science Basis. Contribution of Working Group I to the Fifth Assessment Report on the Intergovernmental Panel on Climate Change, Cambridge University Press, Cambridge, United Kingdom and New York, New York, United States of America, 1535 pp., 2013.

Mercado, L. M., Bellouin, N., Sitch, S., Boucher, O., Huntingford, C., Wild, M. and Cox, P. M.: Impact of changes in diffuse radiation on the global land carbon sink, Nature, 458, 1014-U87, doi:10.1038/nature07949, 2009.

Meehl, G. A., T. F. Stocker, W. D. Collins, P. Friedlingstein, A. T. Gaye, J. M. Gregory, A. Kitoh, R. Knutti, J. M. Murphy, A. Noda, S. C. B. Raper, I. G. Watterson, A. J. Weaver and Z.-C. Zhao: Global Climate Projections. In: Climate Change 2007: The Physical Science Basis. Contribution of Working Group I to the Fourth Assessment Report of the Intergovernmental Panel on Climate Change [Solomon, S., D. Qin, M. Manning, Z. Chen, M. Marquis, K. B. Averyt, M. Tignor and H. L. Miller (eds.)], Cambridge University Press, Cambridge, United Kingdom and New York, NY, USA., 2007.

Sitch, S., Cox, P. M., Collins, W. J. and Huntingford, C.: Indirect radiative forcing of climate change through ozone effects on the land-carbon sink, Nature, 448, 791-U4, doi:10.1038/nature06059, 2007.

Sitch, S., Huntingford, C., Gedney, N., Levy, P. E., Lomas, M., Piao, S. L., Betts, R., Ciais, P., Cox, P., Friedlingstein, P., Jones, C. D., Prentice, I. C. and Woodward, F. I.: Evaluation of the terrestrial carbon cycle, future plant geography and climate-carbon cycle feedbacks using five Dynamic Global Vegetation Models (DGVMs), Glob. Change Biol., 14, 2015-2039, doi: 10.1111/j.1365-2486.2008.01626.x, 2008.